A Precision Search for Exotic Scalar and Tensor Couplings in the Beta Decay of Polarized ^{37}K

by

Melissa Anholm

A Thesis submitted to the Faculty of Graduate Studies of
The University of Manitoba
in partial fulfillment of the requirements of the degree of

DOCTOR OF PHILOSOPHY

Department of Physics and Astronomy
University of Manitoba
Winnipeg

Abstract

Abstract Goes Here

Acknowledgements

People to acknowledge here include: John Behr, Gerald Gwinner, Dan Melconian. Also: Spencer Behling, Ben Fenker. Also-also: Alexandre Gorelov, James McNeil.

Contents

Abstract ii

Acknowledgements iii

Contents vi

List of Figures vii

List of Tables viii

Shit To Do x

1 Background and Motivation 1
- 1.1 Exotic Couplings . . . 1
- 1.2 Fierz Interference – The Physical Signature . . . 1
- 1.3 Present Limits . . . 1
- 1.4 A Toy Experiment . . . 1

2 Theoretical Overview 2
- 2.1 The Basics of Beta Decay . . . 2
- 2.2 JTW Formalism . . . 3
- 2.3 Holstein Formalism . . . 3
- 2.4 Relation between JTW and Holstein Formalisms . . . 3

3 The Experimental Setup 4
- 3.1 Overview . . . 4
- 3.2 AC-MOT and Polarization Setup . . . 6
- 3.3 Measurement Geometry and Detectors . . . 9

4 Calibrations 11
- 4.1 Cloud Measurements via Photoionization . . . 11
- 4.2 Beta Detectors . . . 12
- 4.3 The eMCP . . . 12

5 The Experimental Signature **13**
5.1 The Superratio and Asymmetry . . . 13
5.2 Signature of a Fierz Term in This Experiment . . . 13
5.3 Comparative Merits of the Superratio and Supersum for Measurement 13

6 Estimating Systematic Effects **14**
6.1 Low-energy Scintillator Threshold . . . 14
6.2 BB1 Radius, Energy Threshold, Agreement . . . 14
6.3 Background Modeling . . . 14
6.3.1 Decay from Chamber Surfaces . . . 14
6.4 Quantifying the Effects Backscatter with Geant4 . . . 14
6.5 Lineshape Reconstruction . . . 15
6.5.1 Motivation . . . 15
6.5.2 What is it and how does it work? . . . 15
6.5.3 The Math-Specifics . . . 15
6.5.4 The Results – Things That Got Evaluated This Way . . . 15
6.5.5 The low-energy tail uncertainty, and what it does . . . 15

7 Results **16**
7.1 Measured Limits on b_{Fierz}, C_S, C_T . . . 16
7.2 Discussion of Corrections and Uncertainties . . . 16
7.3 Relation to Other Measurements and New Overall Limits . . . 16

Bibliography **17**

Appendices **19**

A Notable Differences in Data Selection between this and the Previous Result **19**
A.1 Polarization Cycle Selection . . . 19
A.2 Leading Edge / Trailing Edge and Walk Correction . . . 19
A.3 TOF Cut + Background Modelling . . . 20

B Comparing Notation between Holstein and JTW **21**

C Fucking Duh **22**
C.1 The Center of Gravity . . . 22
C.2 Diagonalizing the Hamiltonian . . . 22
C.3 Rotating Coordinates . . . 23
C.4 Lifetimes and Half-Lifes . . . 23
C.5 Reduced Matrix Elements . . . 24
C.6 Doppler Cooling Limit . . . 24

D Misc. Nuclear Physics **25**
D.1 Scalars . . . 25
D.2 Vectors . . . 25
D.3 Axial Vectors . . . 25
D.4 Pseudoscalars . . . 26
D.5 Tensors . . . 26
D.6 Comments on Parity Conservation . . . 26
D.7 Q-Values . . . 26
D.8 Helicity . . . 27
D.9 Conserved Vector Current Hypothesis . . . 27

E Notation **28**
E.1 Things. . . . 28
E.2 Things.2 . . . 29
E.3 Things.3 . . . 30
E.4 Beta End-point Energy . . . 31
E.5 Beta End-point Energy.2 . . . 32

F SuperRatio **33**

G Super Corrections **36**

H How To Lifetime **39**
H.1 Intro . . . 39
H.2 Now What? . . . 40
H.3 After Picking Something... . . . 41

I A PDF **42**
I.1 JTW . . . 42
I.2 Holstein . . . 42

J Holstein/JTW Comparison Confusion **47**

K Multipole Comparisons **52**

L An R_{slow} Thesis Proposal **56**
L.1 An Old Rslow Abstract . . . 56
L.2 Motivation . . . 57
L.3 The Principle of the Measurement . . . 57
L.4 The Decay Process . . . 58
L.5 Current Status . . . 59

List of Figures

3.1 The TRINAT experimental set-up utilizes a two MOT system in order to reduce background in the detection chamber. 5

3.2 The TRINAT detection chamber 6

3.2a A decay event within the TRINAT science chamber. After a decay, the daughter will be unaffected by forces from the MOT. Positively charged recoils and negatively charged shake-off electrons are pulled towards detectors in opposite directions. Although the β^+ is charged, it is also highly relativistic and escapes the electric field with minimal perturbation. 6

3.2b Inside the TRINAT science chamber. This photo is taken from the vantage point of one of the microchannel plates, looking into the chamber towards the second microchannel plate. The current-carrying copper Helmholtz coils and two beta telescopes are visible at the top and bottom. The metallic piece near the center is one of the electrostatic 'hoops' used to generate an electric field within the chamber. The hoop's central circular hole allows access to the microchannel plate, and the two elongated holes on the sides allow the MOT's trapping lasers to pass unimpeded at an angle of 45 degress 'out of the page'. . . 6

3.3 An alternating-current magneto-optical trap with a duty cycle optimized for producing polarized atoms 8

3.3a Components of a magneto-optical trap, including current-carrying magnetic field coils and counterpropagating circularly polarized laser beams. 8

3.3b One cycle of trapping with the AC-MOT, followed by optical pumping to spin-polarize the atoms. After atoms are transferred into the science chamber, this cycle is repeated 500 times before the next transfer. The magnetic dipole field is created by running parallel (rather than anti-parallel as is needed for the MOT) currents through the two coils. 8

List of Tables

Shit To Do

- Is this even true? The pointlike thing? . . . 2
- Is it definitely zirconium? I don't remember. . . . 4
- Probably describe the laser transfer method slightly. . . . 4
- Below is pretty vague. I could do better, even for just an overview-summary thing. Obvs I have to describe it in detail later on *somewhere*, though maybe not in the overview-summary... . . . 5
- Is that ↑ even true?? Because I'm really not sure it is. Via Kofoedhansen, $(E_0 - E_e) = E_\nu$. So there. . . . 7
- Does this work? It really should. . . . 7
- Note that because the atoms within a MOT can be treated as following a thermal distribution, some fraction of the fastest atoms continuously escape from the trap's potential well. Even with the most carefully-tuned apparatus, the AC-MOT cannot quite match a similar standard MOT in terms of retaining atoms. The TRINAT AC-MOT has a 'trapping half-life' of around 6 seconds, and although that may not be particularly impressive by the standards of other MOTs, it is more than adequate for our purposes. ^{37}K itself has a radioactive half-life of only 1.6 seconds (cite someone), so our dominant loss mechanism is radioactive decay rather than thermal escape. . . . 7
- Trap position – Measured using the same dataset that was used to quantify the polarization. The trap drifts slightly over the course of our data collection. Describe the rMCP calibration needed to extract this info. . . 12
- Polarization measurement was conducted on a different set of data, collected in between the measurements used for A_β and b_{Fierz}, and at a higher electric field, because we were unable to run both our MCP detectors simultaneously. . . . 12

Is that ↑ even true?? Because I'm really not sure it is. Via Kofoedhansen, $(E_0 - E_e) = E_\nu$. So there. 32
A thing that's worth noting is that (I think!) recoil-order corrections have been implicitly excluded at some point here. ...Is this even true?? 32

Chapter 1

Background and Motivation

1.1 Exotic Couplings

In particular, we're interested in so-called scalar and tensor couplings within the nuclear weak force. Standard model beta decay involves only vector and axial-vector couplings.

1.2 Fierz Interference – The Physical Signature

The physical effects resulting from the presence of scalar or tensor couplings include a small perturbation to the energy spectrum of betas produced by radioactive decay.

1.3 Present Limits

A bit about other people's physics.

1.4 A Toy Experiment

A quick overview of how an experiment like this one would be set up to extract the physics of interest, to keep the reader from getting too lost in the rest of the thesis.

Chapter 2

Theoretical Overview

2.1 The Basics of Beta Decay

Standard Model beta decay is well understood. The Fermi model of beta decay is in all the textbooks, but you have to dig slightly harder to understand Gamow-Teller or mixed decays, all of which are relevant here.

via Krane [**?**] Under the Allowed Approximation, we require that a beta decay may not carry away any orbital angular momentum, because we treat the nucleus as pointlike and work in the CM frame. An Allowed decay can, however, change the total nuclear angular momentum, because the outgoing leptons have spin= 1/2 and therefore carry angular momentum. Therefore, in an allowed decay, the total nuclear angular momentum must always change by either 0 or 1.

Is this even true? The pointlike thing?

From a 2006 paper by Severijns et al [1], the selection rules for an allowed transition are:

$$\Delta I = I_f - I_i = \{0, \pm 1\} \tag{2.1}$$

$$\hat{\Pi}_i \hat{\Pi}_f = +1 \tag{2.2}$$

Then, you can separate the allowed transitions into singlet (anti-parallel lepton spins, $S = 0$ – a Fermi transition) and triplet states (parallel lepton spins, $S = 1$ – a Gamow-Teller transition).

Fermi decays are so-called "vector" interactions, and happen when the spin of the

two leptons involved are antiparallel, so there can be no change in angular momentum (at least in the case of the Allowed approximation).

Gamow-Teller decays involve two leptons with parallel spins, so the decay must change the projection of the nuclear angular momentum, M_I, by exactly one unit (in the case of the Allowed approximation). They transition may or may not simultaneously change the total nuclear spin, I, by one unit. These are "axial-vector" interactions. (Note that $I = 0 \rightarrow I = 0$ interactions are never Gamow-Teller decays.

Probably everything in this section is yoinked from [**?**], pg 212.

2.2 JTW Formalism

Describes how to search for a variety of BSM terms within beta decay. Does not account for certain well-understood effects of similar (or greater) magnitude.

2.3 Holstein Formalism

An in-depth mathematical description of beta decay, including many smaller effects. It does not include a description of the BSM physics of greatest interest to us.

2.4 Relation between JTW and Holstein Formalisms

To conduct a precision search for scalar and tensor couplings, it is necessary to combine the Holstein and JTW models into a single cohesive probability distribution.

Chapter 3

The Experimental Setup

3.1 Overview

The experimental subject matter of this thesis was conducted at TRIUMF using the apparatus of the TRIUMF Neutral Atom Trap (TRINAT) collaboration. The TRINAT laboratory offers an experimental set-up which is uniquely suited to precision tests of Standard Model beta decay physics, by virtue of its ability to produce highly localized samples of isotopically pure cold atoms within an open detector geometry.

The TRINAT lab accepts radioactive ions delivered by the ISAC beamline at TRIUMF. These ions are collected on the surface of a hot zirconium foil where they are electrically neutralized, and subsequently escape from the foil into the first of two experimental chambers (the "collection chamber"). Within the collection chamber, atoms of one specific isotope – for the purposes of this thesis, ^{37}K – are continuously collected into a magneto-optical trap (MOT). Approximately once per second, the atoms in the collection MOT are transferred to a second experimental chamber (the "detection chamber") and loaded into a second MOT (see Fig. 3.1). Because the transfer and trapping mechanisms rely on tuning to specific atomic resonances, this setup allows for the selection of only a single isotope within the detection MOT, and a significantly reduced background relative to the initial beamline output. The transfer methodology is discussed in some detail within another publication [2].

Is it definitely zirconium? I don't remember.

Probably describe the laser transfer method slightly.

Once the newly transferred atoms have arrived at the second trap, the MOT cycles 500 times between a state where it is 'on' and actively confining atoms to a

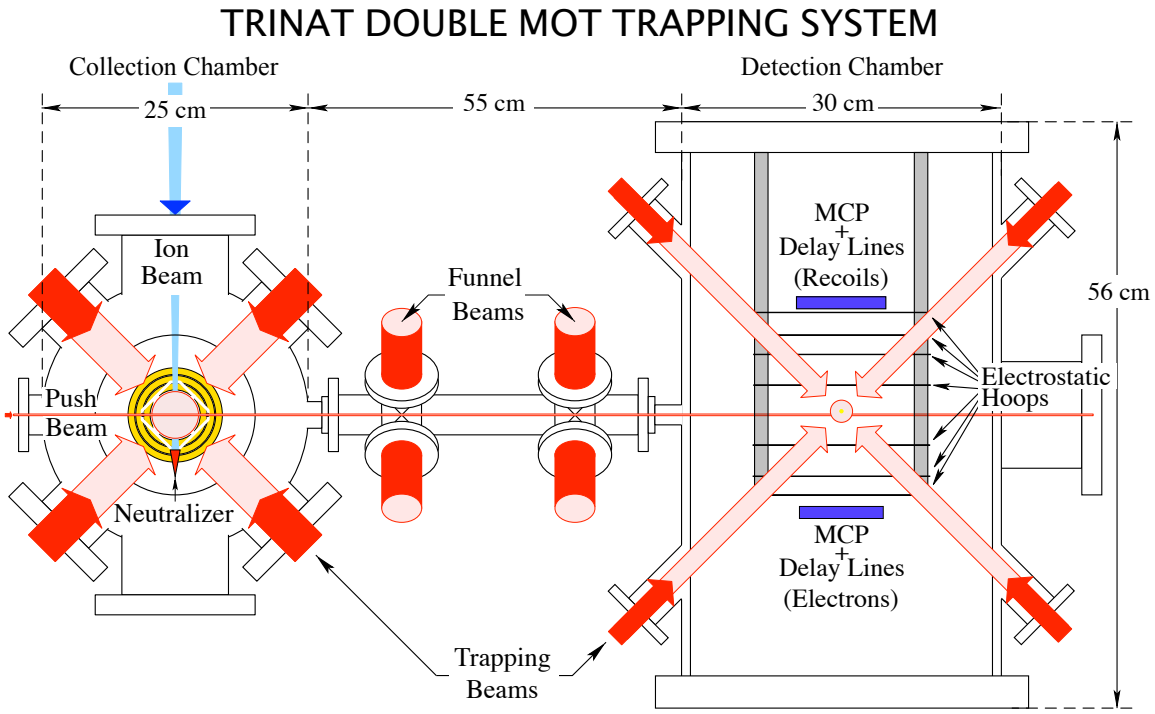

Figure 3.1: The TRINAT experimental set-up utilizes a two MOT system in order to reduce background in the detection chamber.

region of approximately $2\,\mathrm{mm}^3$, to a state where it is 'off' and instead the atoms are spin-polarized by optical pumping while the atom cloud expands ballistically before being re-trapped. In order to eliminate systematic effects, the polarization direction is flipped every 16 seconds. This optical pumping technique and its results are the subject of a recent publication [3].

Below is pretty vague. I could do better, even for just an overview-summary thing. Obvs I have to describe it in detail later on *somewhere*, though maybe not in the overview-summary...

Detectors are positioned about the second MOT for data collection. The science chamber (shown in Figure 3.2) operates at ultra-high vacuum (UHV) and provides the apparatus necessary to intermittently confine atoms within a MOT and then spin-polarize them, and quantify their position, temperature, and initial polarization, and electrostatic hoops to allow for collection and observation of charged recoiling daughter nuclei, as well as further detectors to observe the outgoing betas and reconstruct angular correlations.

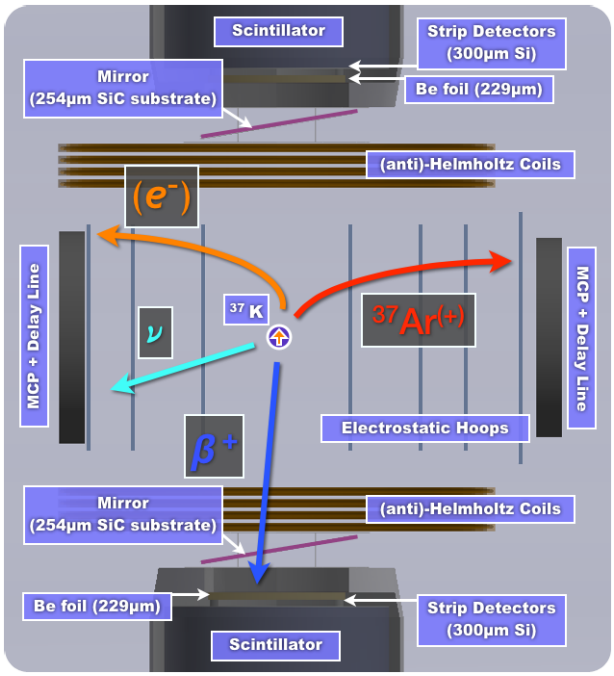

(3.2a) A decay event within the TRINAT science chamber. After a decay, the daughter will be unaffected by forces from the MOT. Positively charged recoils and negatively charged shake-off electrons are pulled towards detectors in opposite directions. Although the β^+ is charged, it is also highly relativistic and escapes the electric field with minimal perturbation.

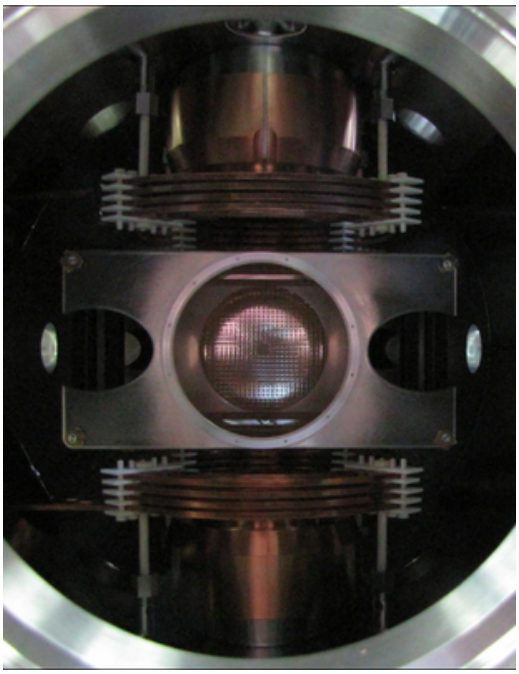

(3.2b) Inside the TRINAT science chamber. This photo is taken from the vantage point of one of the microchannel plates, looking into the chamber towards the second microchannel plate. The current-carrying copper Helmholtz coils and two beta telescopes are visible at the top and bottom. The metallic piece near the center is one of the electrostatic 'hoops' used to generate an electric field within the chamber. The hoop's central circular hole allows access to the microchannel plate, and the two elongated holes on the sides allow the MOT's trapping lasers to pass unimpeded at an angle of 45 degress 'out of the page'.

Figure 3.2: The TRINAT detection chamber

3.2 AC-MOT and Polarization Setup

In order to facilitate a measurement of A_β, we went to great efforts to polarize the atom cloud, and quantify that polarization. This resulted in a duty cycle in which the atoms were intermittently trapped in the AC-MOT, then optically pumped to

polarize them. While knowledge of the polarization is less critical in a measurement of b_{Fierz}, we still use only the polarized portion of the duty cycle in order to minimize other systematic errors, such as the scintillator energy calibration and overall trap position.

Is that $\uparrow$ even true?? Because I'm really not sure it is. Via Kofoedhansen, $(E_0 - E_e) = E_\nu$. So there.

Anyway, here's some figures. Or possibly one figure. Whatever. Also, here's a reference to a figure. See Fig. 3.3, or also its subfigures, eg Fig. 3.3b and Fig. 3.3a. Maybe I have to subref them? Like, eg, Subfig. 3.3b and Subfig. 3.3a. What if we try to subref everything? Consider, eg, Fig. **??**.

Does this work? It really should.

The Magneto-Optical Trap is a well-known technique from atomic physics, used to confine and cool neutral atoms [4]. The technique is used predominantly with alkalis due to their simple orbital electron structure, and is quite robust, so is appropriate for use with ^{37}K. Once set up, the trapping force is specific to the isotope for which the trap has been tuned, which makes it ideal for use in radioactive decay experiments, since the daughters are unaffected by the trapping forces keeping the parent confined.

There are two primary components necessary for any MOT: a laser, and a magnetic field. The laser, which must be circularly polarized in the appropriate directions and tuned slightly to the red of an atomic resonance, is split into three perpendicular retroreflected beams, doppler cooling the atoms and (with the appropriate magnetic field) confining them in all three dimensions (see Figure 3.3a). The TRINAT science chamber includes 6 'viewports' specifically designed to be used for the trapping laser.

A MOT also requires a quadrupolar magnetic field, which we generate with two current-carrying anti-Helmholtz coils located within the vacuum chamber itself. The coils themselves are hollow, and are cooled continuously by pumping temperature-controlled water through them.

One feature which makes our MOT unusual has been developed as a result of our need to rapidly cycle the MOT on and off – that is, it is an "AC-MOT". Rather than running the trap with one particular magnetic field and one set of laser polarizations to match, we run a sinusoidal AC current in the magnetic field coils, and so the sign and magnitude of the magnetic field alternate smoothly between two extrema, and the trapping laser polarizations are rapidly swapped to remain in sync with the field [5][6]. See Figure 3.3b.

Note that because the atoms within a MOT can be treated as following a thermal distribution, some fraction of the fastest atoms continuously escape from the trap's potential well. Even with the most carefully-tuned apparatus, the AC-MOT cannot quite match a similar standard MOT in terms of retaining atoms. The TRINAT AC-MOT has a 'trapping half-life' of around 6 seconds, and although that may not be particularly impressive by the standards of other MOTs, it is more than adequate for our purposes. ^{37}K itself has a radioactive half-life of only 1.6 seconds (cite someone), so our dominant loss mechanism is radioactive decay rather than thermal escape.

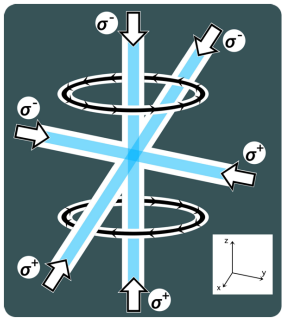

(3.3a) Components of a magneto-optical trap, including current-carrying magnetic field coils and counterpropagating circularly polarized laser beams.

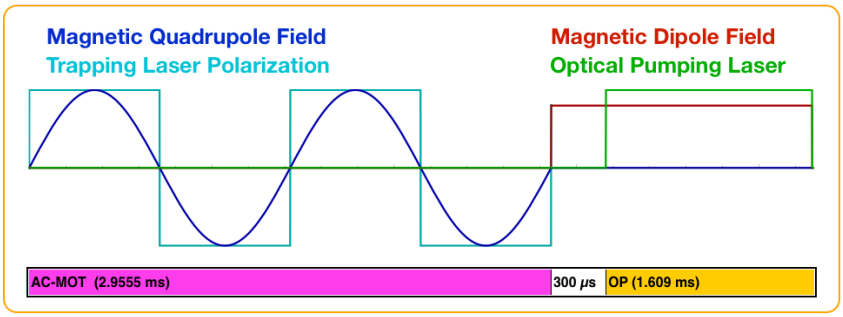

(3.3b) One cycle of trapping with the AC-MOT, followed by optical pumping to spin-polarize the atoms. After atoms are transferred into the science chamber, this cycle is repeated 500 times before the next transfer. The magnetic dipole field is created by running parallel (rather than anti-parallel as is needed for the MOT) currents through the two coils.

Figure 3.3: An alternating-current magneto-optical trap with a duty cycle optimized for producing polarized atoms

We spin-polarize ^{37}K atoms within the trapping region by optical pumping [3]. A circularly polarized laser is tuned to match the relevant atomic resonances, and is directed through the trapping region along the vertical axis in both directions. When a photon is absorbed by an atom, the atom transitions to an excited state and its total angular momentum (electron spin + orbital + nuclear spin) along the vertical axis is incremented by one unit. When the atom is de-excited a photon is emitted isotropically, so it follows that if there are available states of higher and lower angular momentum, the *average* change in the angular momentum projection is zero. If the atom is not yet spin-polarized, it can absorb and re-emit another photon, following a biased random walk towards complete polarization.

In order to optimally polarize a sample of atoms by this method, it is necessary to have precise control over the magnetic field. This is because absent other forces, a spin will undergo Larmor precession about the magnetic field lines. In particular, the magnetic field must be aligned along the polarization axis (otherwise the tendency will be to actually depolarize the atoms), and it must be uniform in magnitude over the region of interest (otherwise its divergencelessness will result in the field also having a non-uniform direction, which results in a spatially-dependent depolarization mechanism). Note that this type of magnetic field is not compatible with the MOT, which requires a quadrupolar magnetic field *gradient*, and has necessitated our use of the AC-MOT as described in Subsection **??**.

3.3 Measurement Geometry and Detectors

Needs several diagrams. Back-to-back beta detectors along the polarization axis. Back-to-back MCPs in an electric field to tag events from the trap, and to measure the trap position and polarization. Hoops to produce the electric field. Many laser ports to make the MOT functional, and for optical pumping. Fancy mirror geometry to combine optical pumping and trapping light along the vertical axis. Water-cooled (anti-)Helmholz coils within the chamber for the AC-MOT, fast switching to produce an optical pumping field.

The beta detectors, located above and below the atom cloud along the axis of polarization (see Figure 3.2a), are each the combination of a plastic scintillator and a set of silicon strip detectors. Using all of the available information, these detectors are able to reconstruct the energy of an incident beta, as well as its hit position, and provide a timestamp for the hit's arrival. Together the upper and lower beta detectors subtend approximately 1.4% of the total solid angle as measured with respect to the cloud position.

It must be noted that the path between the cloud of trapped atoms and either beta detector is blocked by two objects: a 254 μm silicon carbide mirror (necessary for both trapping and optical pumping), and a 229 μm beryllium foil (separating the UHV vacuum within the chamber from the outside world). In order to minimize beta scattering and energy attenuation, these objects have had their materials selected to use the lightest nuclei with the desired material properties, and have been man-

ufactured to be as thin as possible without compromising the experiment. As the $^{37}\mathrm{K} \rightarrow {}^{37}\mathrm{Ar} + \beta^+ + \nu_e$ decay proceess releases $Q = 5.125\,\mathrm{MeV}$ of kinetic energy [7], the great majority of betas are energetic enough to punch through both obstacles without significant energy loss before being collected by the beta detectors.

On opposing sides of the chamber, and perpendicular to the axis of polarization, two stacks of $\sim 80\,\mathrm{mm}$ diameter microchannel plates (MCPs) have been placed (see Figure 3.2) as detectors, providing a time stamp when a particle is incident on their surfaces. Behind each stack of MCPs there is a set of delay lines, which provide position sensitivity for these detectors.

In order to make best use of these MCPs, we create an electric field in order to draw positively charged particles into one MCP, while drawing negatively charged electrons into the other MCP. Seven electrostatic hoops have been placed within the chamber (see Figure 3.2), and are connected to a series of high voltage power supplies. See Sections 4.1 and L.4 for a discussion of what sort of charged particles we expect to observe in these detectors and how they are created.

Scientific data has been collected at field strengths of 395 V/cm, 415 V/cm, and 535 V/cm. It should be noted that these field strengths are too low to significantly perturb any but the least energetic of the (positively charged) betas from the decay process, and these low energy betas would already have been unable to reach the upper and lower beta detectors due to interactions with materials in the SiC mirror and Be foil vacuum seal.

Chapter 4

Calibrations

4.1 Cloud Measurements via Photoionization

In order to measure properties of the trapped ^{37}K cloud, a 10 kHz pulsed laser at 355 nm is directed towards the cloud. These photons have sufficient energy to photoionize neutral ^{37}K from its excited atomic state, releasing 0.77 eV of kinetic energy, but do not interact with ground state ^{37}K atoms. The laser is of sufficiently low intensity that the great majority of excited state atoms are *not* photoionized, so the technique is only very minimally destructive.

Because an electric field has been applied within this region (see Section **??**) the $^{37}K^+$ ions are immediately pulled into the detector on one side of the chamber, while the freed e^- is pulled towards the detector on the opposite side of the chamber. Because $^{37}K^+$ is quite heavy relative to its initial energy, it can be treated as moving in a straight line directly to the detector, where its hit position on the microchannel plate is taken as a 2D projection of its position within the cloud. Similarly, given a sufficient understanding of the electric field, the time difference between the laser pulse and the microchannel plate hit allows for a calculation of the ion's initial position along the third axis.

With this procedure, it is possible to produce a precise map of the cloud's position and size, both of which are necessary for the precision measurements of angular correlation parameters that are of interest to us here. However, it also allows us to extract a third, slightly more subtle and significantly more important measurement: the cloud's *polarization*.

The key to the polarization measurement is that only atoms in the excited atomic state can be photoionized. While the MOT runs, atoms are constantly being pushed around and excited by the trapping lasers, so this period of time provides a lot of information for characterizing the trap size and position. When the MOT is shut off, the atoms quickly return to their ground states and are no longer photoionized until the optical pumping beam is turned on. As described in Section **??**, and in greater detail in [3], the optical pumping process involves repeatedly exciting atoms from their ground states until the atoms finally cannot absorb any further angular momentum and remain in their fully-polarized (ground) state until they are perturbed. Therefore, there is a sharp spike in excited-state atoms (and therefore photoions) when the optical pumping begins, and none once the cloud has been completely polarized. The number of photoion events that occur once the sample has been maximally polarized, in comparison with the size and shape of the initial spike of photoions, provides a very precise characterization of the cloud's final polarization [3].

Trap position – Measured using the same dataset that was used to quantify the polarization. The trap drifts slightly over the course of our data collection. Describe the rMCP calibration needed to extract this info.

Polarization measurement was conducted on a different set of data, collected in between the measurements used for A_β and b_{Fierz}, and at a higher electric field, because we were unable to run both our MCP detectors simultaneously.

4.2 Beta Detectors

Energy calibration for the scintillator+PMT setup changed dramatically at one point. Describe how calibration was done. Also describe how the DSSD calibration was done, even though it wasn't implemented by me.

4.3 The eMCP

I can describe the eMCP calibration here, even though it mostly wasn't implemented by me. It is tangentially relevant to data selection and background estimation by providing an experimental energy spectrum for shake-off electrons.

Chapter 5

The Experimental Signature

5.1 The Superratio and Asymmetry

The data can be combined into a superratio asymmetry. This has the benefit of causing many systematics to cancel themselves out at leading order. It also will increase the fractional size of the effects we're looking for. This can be shown by using math.

5.2 Signature of a Fierz Term in This Experiment

Not all systematics effects are eliminated. We'll want to be careful to propagate through any effects that are relevant. Using the superratio asymmetry as our physical observable makes this process a bit messier for the things that don't cancel out, but it's all just math.

5.3 Comparative Merits of the Superratio and Supersum for Measurement

Some other groups have performed similar measurements using the supersum as the physical observable. There are pros and cons to both methods. I can show, using a back-of-the-envelope calculation, that for this particular dataset, the superratio asymmetry method produces a better result.

Chapter 6

Estimating Systematic Effects

6.1 Low-energy Scintillator Threshold

Choice of low-energy scintillator threshold has a large systematic effect...

6.2 BB1 Radius, Energy Threshold, Agreement

BB1 radius cut can help to eliminate scattered events. Energy threshold selection and statistical agreement between BB1 detectors' energies only makes a small effect on results.

6.3 Background Modeling

6.3.1 Decay from Chamber Surfaces

6.4 Quantifying the Effects Backscatter with Geant4

Beta decay (back-)scatter from surfaces within the experimental chamber is a significant systematic, and it must be evaluated, quantified, and corrected for. This is done via a series of GEANT4 simulations. While only a small fraction of events are affected, the process results in an energy loss in the beta that can, if not understood, be misinterpreted as the exact signal we're searching for. It is therefore imperative that this be well understood.

6.5 Lineshape Reconstruction

6.5.1 Motivation

This process is used because the (back-)scatter, which it itself an important systematic, is largely independent of a wide variety of other experimental effects. These other effects must all be evaluated, but it is computationally prohibitive to re-evaluate the scattering with every other effect under consideration.

6.5.2 What is it and how does it work?

Mono-energetic beta decay events are generated in GEANT4, which outputs an energy spectrum for unscattered and forward-scattered beta events in the detector. These spectra are fit to a function to model the scintillator resolution, as well as energy loss in materials that the beta passed through before arriving at the scintillator. These spectrum fits are performed for a set of beta energies, and parameters are extrapolated to be applied to betas emitted at intermediate energies. Thus, the whole spectrum can be modeled. Pictures will make this clearer.

6.5.3 The Math-Specifics

I'll write down the specific functions I'm using, and the parameter values I'm using. (Maybe this should go in an appendix instead?) I'll describe the adjustments I make to the spectrum so that it can work even for the dataset where the scintillators' resolutions have changed.

6.5.4 The Results – Things That Got Evaluated This Way

Trap position, size, sail velocity. Thicknesses of the SiC mirror, the Be foil, and the DSSD. Scintillator calibration.

6.5.5 The low-energy tail uncertainty, and what it does

Chapter 7

Results

7.1 Measured Limits on b_{Fierz}, C_S, C_T

Results go here, with measured limits described and quantified in all formats anyone could ever care about.

7.2 Discussion of Corrections and Uncertainties

...

7.3 Relation to Other Measurements and New Overall Limits

In which I'll show exclusion plots and write down new limits, combining my result with results from the literature.

Bibliography

[1] Severijns, N., Beck, M. and Naviliat-Cuncic, O., *Tests of the standard electroweak model in nuclear beta decay*, Rev. Mod. Phys., Vol. 78, pp. 991–1040, September 2006.

[2] Swanson, T. B., Asgeirsson, D., Behr, J. A., Gorelov, A. and Melconian, D., *Efficient transfer in a double magneto-optical trap system*, J. Opt. Soc. Am. B, Vol. 15, No. 11, pp. 2641–2645, Nov 1998.

[3] Fenker, B., Behr, J. A., Melconian, D., Anderson, R. M. A., Anholm, M., Ashery, D., Behling, R. S., Cohen, I., Craiciu, I., Donohue, J. M., Farfan, C., Friesen, D., Gorelov, A., McNeil, J., Mehlman, M., Norton, H., Olchanski, K., Smale, S., Thériault, O., Vantyghem, A. N. and Warner, C. L., *Precision measurement of the nuclear polarization in laser-cooled, optically pumped* ^{37}K, New Journal of Physics, Vol. 18, No. 7, pp. 073028, 2016.

[4] Raab, E. L., Prentiss, M., Cable, A., Chu, S. and Pritchard, D. E., *Trapping of Neutral Sodium Atoms with Radiation Pressure*, Phys. Rev. Lett., Vol. 59, pp. 2631–2634, Dec 1987.

[5] Harvey, M. and Murray, A. J., *Cold Atom Trap with Zero Residual Magnetic Field: The AC Magneto-Optical Trap*, Phys. Rev. Lett., Vol. 101, pp. 173201, Oct 2008.

[6] Anholm, M., Characterizing the AC-MOT, Master's thesis, University of British Columbia, 2014.

[7] Audi, G., Wapstra, A. and Thibault, C., *The AME2003 Atomic Mass Evaluation*, Nuclear Physics A, Vol. 729, No. 1, pp. 337 – 676, 2003.

[8] Severijns, N. and Naviliat-Cuncic, O., *Symmetry tests in nuclear beta decay*, Annual Review of Nuclear and Particle Science, Vol. 61, pp. 23–46, 2011.

[9] Jackson, J. D., Treiman, S. B. and Wyld, H. W., *Possible Tests of Time Reversal Invariance in Beta Decay*, Phys. Rev., Vol. 106, pp. 517–521, May 1957.

[10] Jackson, J. D., Treiman, S. B. and Wyld, H. W., *Coulomb Corrections in Allowed Beta Transitions*, Nuclear Physics, Vol. 4, pp. 206–212, Nov. 1957.

[11] Gorelov, A., Behr, J., Melconian, D., Trinczek, M., Dubé, P., Häusser, O., Giesen, U., Jackson, K., Swanson, T., D'Auria, J., Dombsky, M., Ball, G., Buchmann, L., Jennings, B., Dilling, J., Schmid, J., Ashery, D., Deutsch, J., Alford, W., Asgeirsson, D., Wong, W. and Lee, B., *Beta–neutrino correlation experiments on laser trapped* ^{38m}K, ^{37}K, Hyperfine Interactions, Vol. 127, No. 1, pp. 373–380, 2000.

[12] Melconian, D. G., Measurement of the Neutrino Asymmetry in the Beta Decay of Laser-Cooled, Polarized ^{37}K, Ph.D. thesis, Simon Fraser University, 2005.

Appendix A

Notable Differences in Data Selection between this and the Previous Result

A.1 Polarization Cycle Selection

Data used for our recent PRL article was slightly less polarized than we thought it was, due to an oversight in the data selection procedure.

A.2 Leading Edge / Trailing Edge and Walk Correction

Using the leading edge rather than the trailing edge to mark the timing of TDC pulses cleans up jitter, eliminates background, and changes the relative delays between different inputs. It is immediately relevant to the shape of the 'walk correction' on scintillator timing pulses, which give a different prediction for beta arrival time as a function of scintillator energy.

A.3 TOF Cut + Background Modelling

A SOE-beta time-of-flight cut is necessary to reduce background. The above mentioned walk correction directly results in an change in which specific events are selected in a given TOF cut. It further results in an adjustment to the expected fraction of background events in any such cut.

Appendix B

Comparing Notation between Holstein and JTW

This is a short guide to differences in notation, sign convention, and normalization. There will be many tables here, chosen to aid in conversion between the two conventions.

Appendix C

Things that Should Be Very Fucking Obvious

C.1 The Center of Gravity

It's what happens when you set $A = 0$ and $B = 0$. That is all.

C.2 Diagonalizing the Hamiltonian

Given a Hermitian matrix $\hat{\Omega}$, there exists a unitary matrix $\hat{U}$ such that $\hat{U}^\dagger \hat{\Omega} \hat{U}$ is diagonalized. Solving for this matrix $\hat{U}$ is, in this case, equivalent to solving the eigenvalue problem for $\hat{\Omega}$ [**?**]. As it turns out, $\hat{U}$ is the matrix of eigenvectors of $\hat{\Omega}$, by which I mean that the eigenvectors are column vectors, and they're all squished together to make $\hat{U}$. It doesn't matter what order you put them in, but they probably have to be normalized.

Then, if

$$\hat{\Omega}' := \hat{U}^\dagger \hat{\Omega} \hat{U}, \tag{C.1}$$

we find that $\hat{\Omega}'$ is the diagonal matrix with its elements being the eigenvalues. They're in the same order as the eigenvectors we squished together to make $\hat{U}$ previously.

Also, a unitary operator, $\hat{U}$ is one which satisfies:

$$\hat{U}\hat{U}^\dagger = \hat{U}^\dagger \hat{U} = \underset{\sim}{I}. \tag{C.2}$$

C.3 Rotating Coordinates

If by $\hat{\Omega}$ we really mean the Hamiltonian $\hat{H}$, and by $\hat{U}$ we really mean a coordinate change that takes us to rotating coordinates such that we can easily make a rotating wave approximation, we must take more things into account. In particular, we find that our new rotating-coordinate Hamiltonian, $\tilde{H}$ is given by:

$$\tilde{H} = \hat{U}^{\dagger}\hat{H}\hat{U} - \hbar\hat{A} \tag{C.3}$$

where

$$\hat{U} := e^{-i\hat{A}t}. \tag{C.4}$$

This additional term arises from our statement of the Schrodinger equation,

$$\hat{H}\,|\psi\rangle = i\hbar\frac{\partial}{\partial t}\,|\psi\rangle\,. \tag{C.5}$$

In particular, note that C.5 includes only a partial derivative of the wavefunction. I derive this result explicitly in Chapter **??**. See also Ref. [**?**], pg. 195.

C.4 Lifetimes and Half-Lifes

Since different people use different notation to describe exponential decay of a physical quantity, it is useful to be able to relate two of the most common methods for describing the decay. We begin with the rate equation,

$$\frac{dN}{dt} \;=\; -\gamma\, N, \tag{C.6}$$

where it is clear that the "rate" of decay must be $\gamma\, N$. If we initially have N_0 of the quantity in question, then Eq. C.6 has as its solution

$$N(t) \;=\; N_0\, e^{-\gamma\, t}. \tag{C.7}$$

Note that the physical interpretation of γ is the "linewidth".

We'll wish to convert γ into other quantities of interest. In particular, we can

re-write the solution C.7 as

$$N(t) \;=\; N_0\, e^{-t/\tau}, \tag{C.8}$$

where $\tau = 1/\gamma$ is referred to as the "lifetime". Then, we find the half-life $t_{1/2}$ by enforcing the fact that it is the time at which the number of remaining atoms is equal to half of what was originally present. Therefore,

$$N(t_{1/2}) = N_0 e^{-t_{1/2}/\tau} \;=\; \frac{1}{2}N_0 \tag{C.9}$$

$$e^{-t_{1/2}/\tau} \;=\; 1/2 \tag{C.10}$$

$$t_{1/2}/\tau \;=\; \ln(2). \tag{C.11}$$

Thus, we see that

$$t_{1/2} \;=\; \ln(2)\,\tau, \tag{C.12}$$

where τ is the "lifetime" of the state, and $t_{1/2}$ is its "half-life".

C.5 Reduced Matrix Elements

The Wigner-Eckart Theorem says, for vector operator V^q,

$$\langle \alpha' j' m' | V^q | \alpha j m \rangle = \langle j' m' | j 1 m q \rangle \langle \alpha' j' \| V \| \alpha j \rangle. \tag{C.13}$$

The point being that $\langle \alpha' j' \| V \| \alpha j \rangle$ is the same for all m and q.

C.6 Doppler Cooling Limit

Here it is!

$$kT_{\mathrm{D}} = \frac{1}{2}\hbar\Gamma \tag{C.14}$$

Appendix D

The Parity Operator: Vectors and Axial Vectors and Pseudoscalars, oh my!

via Samuel Wong, 1990. pg 212.

D.1 Scalars

A scalar does not change sign under the parity operation, because why even would it?

D.2 Vectors

Vectors, or "polar vectors" (V) are exactly what I think they are. Position $\vec{r}$ and (linear) momentum $\vec{p}$ are examples. The thing about these vectors is that they change sign (or, really, direction) under a parity transformation.

D.3 Axial Vectors

Axial vectors (A) *don't* change sign under a parity transformation. An example is angular momentum, $\vec{L} = \vec{r} \times \vec{p}$. This is where the "mirror" thing breaks down. A mirror only is only a one-dimensional parity operator, so if you think of a thing

with angular momentum and its reflection in a mirror, you imagine the mirror image with reversed angular momentum too. But in reality, if you change the sign of *all components* of $\vec{r}$ and simultaneously all components of $\vec{p}$, it's clear that the quantity $(\vec{r} \times \vec{p})$ remains unchanged. Pauli spin matrices, $\vec{\sigma}$, are axial vectors.

D.4 Pseudoscalars

Pseudoscalars, (P). You'd think they were scalars, because they're just a number, but have to remember that you got them by taking the scalar product of a (polar) vector and an axial vector. If you apply the parity operator to the quantity $P = (\vec{V} \cdot \vec{A})$, $\vec{V}$ changes sign (for all components) while $\vec{A}$ does not. So the resultant "scalar" P has to change sign too. That's how you know that P is really a pseudoscalar.

D.5 Tensors

...Yeah, Wong doesn't really get into that. At least not here.

D.6 Comments on Parity Conservation

An interaction made from a mixture of scalars and pseudoscalars, or a mixture of vectors and axial vectors, does *not* conserve parity.

For the strong and electromagnetic forces, parity *is* strictly conserved. Not so for the weak force!

D.7 Q-Values

The Q-value for a particular interaction is defined as the difference between the kinetic energies of the final and initial systems.

$$Q = T_f - T_i \tag{D.1}$$

In particular, for β^+ decay, we're including .... which things? ... as part of the mass of the various systems?

D.8 Helicity

Helicity, h, is a pseudoscalar.

$$h = \frac{\vec{\sigma} \cdot \vec{p}}{|\vec{p}|} \tag{D.2}$$

D.9 Conserved Vector Current Hypothesis

The CVC hypothesis asserts that the Fermi interactions of nucleons within a nucleus are *not* changed by all the surrounding mesons. (What?)

Appendix E

Proposed Notation

E.1 Things.

The jtw expression, after integrating over $d\Omega_\nu$ and making some substitutions (and more controversially, adjustments so that neutrinos aren't massless, and recoil energy isn't zero), turns out like this:

$$
\begin{aligned}
&\omega\mathrm{d(stuff)} \\
&\quad = \; 2\left(\frac{1}{2\pi}\right)^4 p_\beta E_\beta \left(|\vec{p}_\beta + \vec{p}_r|\right)(Q - E_\beta - E_r) dE_\beta d\Omega_\beta \xi \\
&\qquad \times \left[1 + a_{\beta\nu}\left(\frac{-|\vec{p}_\beta|^2 - \vec{p}_\beta \cdot \vec{p}_r}{E_\beta(Q - E_\beta - E_r)}\right) + b_{\mathrm{Fierz}}\left(\frac{m_e}{E_\beta}\right)\right. \\
&\qquad + c_{\mathrm{align}}\left(\frac{J(J+1) - 3\left\langle(\vec{J}\cdot\hat{j})^2\right\rangle}{J(2J+1)}\right)\left(\frac{-\frac{1}{3}(|\vec{p}_\beta|^2 + \vec{p}_\beta\cdot\vec{p}_r) + (\vec{p}_\beta\cdot\hat{j})^2 + (\vec{p}_\beta\cdot\hat{j})(\vec{p}_r\cdot\hat{j})}{E_\beta(Q - E_\beta - E_r)}\right) \\
&\qquad \left. + \frac{\left\langle\vec{J}\right\rangle}{J}\cdot\left[A_\beta\frac{\vec{p}_\beta}{E_\beta} + B_\nu\left(\frac{-\vec{p}_\beta - \vec{p}_r}{Q - E_\beta - E_r}\right) + D\left(\frac{(\vec{p}_r\times\vec{p}_\beta)}{E_\beta(Q - E_\beta - E_r)}\right)\right]\right]. \qquad \text{(E.1)}
\end{aligned}
$$

Assumptions/substitutions that I made in order to arrive at that expression are:

$$Q = E_\beta + E_\nu + E_r \tag{E.2}$$

$$\vec{p}_\beta + \vec{p}_\nu + \vec{p}_r = 0 \tag{E.3}$$

$$(E_0 - E_e)^2 \to p_\nu E_\nu = |\vec{p}_\beta + \vec{p}_r| \, (Q - E_\beta - E_r) \tag{E.4}$$

$$\int d\Omega_\nu = 4\pi. \tag{E.5}$$

E.2 Things.2

Actually though, I'm'a back up. Let's talk about dot products in spherical coordinates. Of course, in Cartesian coordinates,

$$\vec{p}_\beta = p_\beta \begin{bmatrix} \sin\theta_\beta \cos\phi_\beta \\ \sin\theta_\beta \sin\phi_\beta \\ \cos\theta_\beta \end{bmatrix} ; \quad \vec{p}_r = p_r \begin{bmatrix} \sin\theta_r \cos\phi_r \\ \sin\theta_r \sin\phi_r \\ \cos\theta_r \end{bmatrix} ; \quad \vec{p}_\nu = p_\nu \begin{bmatrix} \sin\theta_\nu \cos\phi_\nu \\ \sin\theta_\nu \sin\phi_\nu \\ \cos\theta_\nu \end{bmatrix} \tag{E.6}$$

and

$$\vec{p}_\beta + \vec{p}_r + \vec{p}_\nu = 0. \tag{E.7}$$

We'd like to find an expression for $\vec{p}_\beta \cdot \vec{p}_\nu$, and we'd probably like to get rid of all dependence on the direction of ν, which will make the integral over $d\Omega_\nu$ easier to deal with.

$$\begin{aligned}
\vec{p}_\beta \cdot \vec{p}_\nu &= -\vec{p}_\beta \cdot (\vec{p}_\beta + \vec{p}_r) && \text{(E.8)} \\
&= -p_\beta^2 - \vec{p}_\beta \cdot \vec{p}_r && \text{(E.9)} \\
&= -p_\beta^2 - p_\beta p_r \begin{bmatrix} \sin\theta_\beta \cos\phi_\beta \\ \sin\theta_\beta \sin\phi_\beta \\ \cos\theta_\beta \end{bmatrix} \cdot \begin{bmatrix} \sin\theta_r \cos\phi_r \\ \sin\theta_r \sin\phi_r \\ \cos\theta_r \end{bmatrix} && \text{(E.10)} \\
&= -p_\beta^2 - p_\beta p_r \left[\sin\theta_\beta \cos\phi_\beta \sin\theta_r \cos\phi_r + \sin\theta_\beta \sin\phi_\beta \sin\theta_r \sin\phi_r \right. \\
&\quad \left. + \cos\theta_\beta \cos\theta_r\right] && \text{(E.11)} \\
&= -p_\beta^2 - p_\beta p_r \left[\cos\theta_\beta \cos\theta_r + \sin\theta_\beta \sin\theta_r \cos(\phi_\beta - \phi_r)\right], && \text{(E.12)}
\end{aligned}$$

where that last step happens via the use of some nice trig identities, and Mathematica confirms it. Equivalently, though:

$$\vec{p}_\beta \cdot \vec{p}_\nu = p_\beta p_\nu \left[\cos\theta_\beta \cos\theta_\nu + \sin\theta_\beta \sin\theta_\nu \cos(\phi_\beta - \phi_\nu)\right]. \tag{E.13}$$

That version is actually probably better, since recoil momentum isn't even a thing, for the purposes of integration.

Consider, now, the integral:

$$\begin{aligned}
\int \frac{\vec{p}_\beta \cdot \vec{p}_\nu}{E_\beta E_\nu} d\Omega_\nu &= \int_0^{2\pi}\int_0^{\pi} \frac{\vec{p}_\beta \cdot \vec{p}_\nu}{E_\beta E_\nu} \sin\theta_\nu d\theta_\nu d\phi_\nu && \text{(E.14)}\\
&= \frac{p_\beta p_\nu}{E_\beta E_\nu} \int_0^{2\pi}\int_0^{\pi} \left[\cos\theta_\beta \cos\theta_\nu + \sin\theta_\beta \sin\theta_\nu \cos(\phi_\beta - \phi_\nu)\right] \sin\theta_\nu d\theta_\nu d\phi_\nu && \text{(E.15)}\\
&= \frac{p_\beta p_\nu}{E_\beta E_\nu} \left[2\pi \cos\theta_\beta \int_0^{\pi} \cos\theta_\nu \sin\theta_\nu d\theta_\nu \right.\\
&\quad \left. + \sin\theta_\beta \int_0^{2\pi} \cos(\phi_\beta - \phi_\nu) \int_0^{\pi} \sin^2\theta_\nu d\theta_\nu d\phi_\nu \right] && \text{(E.16)}\\
&= \frac{p_\beta p_\nu}{E_\beta E_\nu} \frac{\pi}{2} \sin\theta_\beta \int_0^{2\pi} \cos(\phi_\beta - \phi_\nu) d\phi_\nu && \text{(E.17)}\\
&= 0. && \text{(E.18)}
\end{aligned}$$

That obviously didn't work. Probably $p_\nu = p_\nu(\hat{p}_\nu)$. How do I even *deal* with that?!?

–

Actually, according to insight that Alexandre thought was very obvious, because it was, this notation only happened in the first place because the lab frame matters. it's measured w.r.t. polarization or alignment or something. The integration over the two leptons is really an integration over the lab frame + one lepton.

E.3 Things.3

Suppose I integrate jtw over everything but electron energy. What's left?

$$\omega\mathrm{d(stuff)} = \left(\frac{1}{2\pi}\right)^5 (4\pi)^2 \, p_\beta E_\beta E_\nu^2 \, dE_\beta \, \xi \left[1 + b_{\mathrm{Fierz}} \left(\frac{m_e}{E_\beta}\right)\right]. \tag{E.19}$$

...Or, in units that don't suck, with terminology that's useful to us (and assuming massless neutrinos, which is fine, 'cause the uncertainty in Q is like 200 eV or something (check value)),

$$\omega \mathrm{d}(\mathrm{stuff}) \;=\; 4\left(\frac{1}{2\pi}\right)^3 \frac{(E_\beta^2 - m^2c^4)^{1/2}}{c}\, E_\beta (Q - E_\beta - E_{r\mathrm{kin}})^2\, dE_\beta\, \xi \left[1 + b_{\mathrm{Fierz}}\left(\frac{m_e c^2}{E_\beta}\right)\right] \tag{E.20}$$

Integrate over the beta energy (**NOT** between $E_\beta = m_e c^2$ and $E_\beta = m_e c^2 + Q$; fix this in the code!) and we find:

$$\omega \;=\; 4\left(\frac{1}{2\pi}\right)^3 (...) \tag{E.21}$$

This is *probably* interpreted as the overall decay rate, somehow.

E.4 Beta End-point Energy

Note that nuclear physics notational convention, which is fucking retarded, apparently defines kinetic energy T s.t.

$$E = T + mc^2, \tag{E.22}$$

but of course, it's still the case that

$$E = (p^2c^2 + m^2c^4)^{1/2}. \tag{E.23}$$

But since $Q = T_{final} - T_{initial}$, we're sort-of stuck, if we want to describe the beta end-point energy in terms of Q, we find that

$$E_{\mathrm{end}} = Q + m_e c^2 \tag{E.24}$$

$$Q = (p_{\mathrm{max}}^2 c^2 + m_e^2 c^4)^{1/2} - m_e c^2 \tag{E.25}$$

... actually, pretty sure that's all wrong. ... ... Actually-actually, it's fine. See "jtw_integration_scratch3.nb" for more-other details. That version, I believe, finally got all the thingies right.

E.5 Beta End-point Energy.2

Firstly, some Q-values for ^{37}K (via bnl).

$$Q_{\mathrm{EC}} = 6.147\,45(23)\,\mathrm{MeV} \tag{E.26}$$
$$Q_{\beta+} = 5.125\,45(23)\,\mathrm{MeV} \tag{E.27}$$

It would be better if I knew the branching ratio for EC/$\beta+$ though.

Anyway, in the jtw notation,

$$E_0 := Q + m_e c^2. \tag{E.28}$$

Is that ↑ even true?? Because I'm really not sure it is. Via Kofoedhansen, $(E_0 - E_e) = E_\nu$. So there.

What does that mean in terms of the individual particles' energies? Well, if that's the beta end-point energy, it just means that that's the total (kinetic + rest) energy for the beta. So, we can distribute Q of kinetic energy around to the other particles.

$$Q = T_\beta + T_\nu + T_r \tag{E.29}$$
$$= (E_\beta - m_\beta c^2) + (E_\nu - m_\nu c^2) + (E_r - M_r c^2) \tag{E.30}$$
$$\approx E_\beta - m_\beta c^2 + E_\nu + T_r \tag{E.31}$$
$$E_0 \approx E_\beta + E_\nu + T_r \tag{E.32}$$

$$T_\beta = \left(p_\beta^2 c^2 + m_e^2 c^4\right)^{1/2} - m_e c^2 \tag{E.33}$$
$$T_\nu = \left(p_\nu^2 c^2 + m_\nu^2 c^4\right)^{1/2} - m_\nu c^2$$
$$\approx p_\nu c \tag{E.34}$$
$$T_r = \left(p_r^2 c^2 + m_r^2 c^4\right)^{1/2} - m_r c^2$$
$$\approx \frac{p_r^2}{2m_r} \tag{E.35}$$

A thing that's worth noting is that (I think!) recoil-order corrections have been implicitly excluded at some point here. ...Is this even true??

Appendix F

Derivation of the b_{Fierz} Dependence of the Superratio Asymmetry

Consider, from JTW, the probability distribution for outgoing beta particles in terms of only the electron energy and direction w.r.t. parent nuclear polarization (other parameters have been integrated over). We have

$$P(E_\beta) \;=\; W(E_\beta)\left[1 + b_{\mathrm{Fierz}}\frac{mc^2}{E_\beta} + A_\beta\,\frac{v}{c}|\vec{P}|\cos\theta\right]. \tag{F.1}$$

In the TRINAT geometry with two polarization states (+/-) and two detectors (T/B), we are able to describe four different count rates, with different combinations of polarization states and detectors. Thus, we have:

$$r_{\mathrm{T}+}(E_\beta) \;=\; \varepsilon_{\mathrm{T}}(E_\beta)\,\Omega_T\,N_+\left[1 + b_{\mathrm{Fierz}}\frac{mc^2}{E_\beta} + A_\beta\,\frac{v}{c}|\vec{P}_+|\langle\cos\theta\rangle_{\mathrm{T}+}\right] \tag{F.2}$$

$$r_{\mathrm{B}+}(E_\beta) \;=\; \varepsilon_{\mathrm{B}}(E_\beta)\,\Omega_B\,N_+\left[1 + b_{\mathrm{Fierz}}\frac{mc^2}{E_\beta} + A_\beta\,\frac{v}{c}|\vec{P}_+|\langle\cos\theta\rangle_{\mathrm{B}+}\right] \tag{F.3}$$

$$r_{\mathrm{T}-}(E_\beta) \;=\; \varepsilon_{\mathrm{T}}(E_\beta)\,\Omega_T\,N_-\left[1 + b_{\mathrm{Fierz}}\frac{mc^2}{E_\beta} + A_\beta\,\frac{v}{c}|\vec{P}_-|\langle\cos\theta\rangle_{\mathrm{T}-}\right] \tag{F.4}$$

$$r_{\mathrm{B}-}(E_\beta) \;=\; \varepsilon_{\mathrm{B}}(E_\beta)\,\Omega_B\,N_-\left[1 + b_{\mathrm{Fierz}}\frac{mc^2}{E_\beta} + A_\beta\,\frac{v}{c}|\vec{P}_-|\langle\cos\theta\rangle_{\mathrm{B}-}\right], \tag{F.5}$$

where $\varepsilon_{\mathrm{T/B}}(E_\beta)$ are the (top/bottom) detector efficiencies, $\Omega_{\mathrm{T/B}}$ are the fractional solid angles for the (top/bottom) detector from the trap position, $N_{+/-}$ are the number of atoms trapped in each (+/-) polarization state, and $|\vec{P}_{+/-}|$ are the magnitudes

of the polarization along the detector axis for each polarization state. $\langle \cos\theta \rangle_{\mathrm{T/B},+/-}$ is the average of $\cos\theta$ for *observed* outgoing betas, for each detector and polarization state combination. This latter term is approximately ± 1, and contains important sign information. For a pointlike trap in the center of the chamber, 103.484 mm from either (DSSSD) detector, each of which is taken to be circular with a radius of 15.5 mm, we find that $\langle |\cos\theta| \rangle_{\mathrm{T/B},+/-} \approx 0.994484$, and is the same for all four cases (or for $r = 15.0\,\mathrm{mm}$, we find that $\langle |\cos\theta| \rangle_{\mathrm{T/B},+/-} \approx 0.994829$). Note that a horizontally displaced trap will decrease the magnitude of $\langle |\cos\theta| \rangle$, but all four values will remain equal to one another. In the case of a vertically displaced trap, these four values will no longer all be equal, however it will still be the case that $\langle |\cos\theta| \rangle_{\mathrm{T}+} = \langle |\cos\theta| \rangle_{\mathrm{T}-}$, and $\langle |\cos\theta| \rangle_{\mathrm{B}+} = \langle |\cos\theta| \rangle_{\mathrm{B}-}$.

For simplicity, we will henceforth assume that the trap is vertically centered, and take $|\vec{P}_+| = |\vec{P}_-|$. We also define the following:

$$A' = A'(E_\beta) \equiv A_\beta \frac{v}{c} |\vec{P}| \langle |\cos\theta| \rangle \tag{F.6}$$

$$b' = b'(E_\beta) \equiv b_{\mathrm{Fierz}} \frac{mc^2}{E_\beta}, \tag{F.7}$$

and choose a coordinate system in which the + polarization state is, in some sense, 'pointing up' toward the top detector, such that

$$\langle \cos\theta \rangle_{\mathrm{T}+} \approx +1 \tag{F.8}$$

$$\langle \cos\theta \rangle_{\mathrm{B}+} \approx -1 \tag{F.9}$$

$$\langle \cos\theta \rangle_{\mathrm{T}-} \approx -1 \tag{F.10}$$

$$\langle \cos\theta \rangle_{\mathrm{B}-} \approx +1. \tag{F.11}$$

This allows us to rewrite the four count rates in simplified notation, as:

$$r_{\mathrm{T}+} = \varepsilon_{\mathrm{T}} N_+ (1 + b' + A') \tag{F.12}$$

$$r_{\mathrm{B}+} = \varepsilon_{\mathrm{B}} N_+ (1 + b' - A') \tag{F.13}$$

$$r_{\mathrm{T}-} = \varepsilon_{\mathrm{T}} N_- (1 + b' - A') \tag{F.14}$$

$$r_{\mathrm{B}-} = \varepsilon_{\mathrm{B}} N_- (1 + b' + A'). \tag{F.15}$$

We further define the 'superratio', s, to be:

$$s = \frac{r_{\mathrm{T}-}\, r_{\mathrm{B}+}}{r_{\mathrm{T}+}\, r_{\mathrm{B}-}}. \tag{F.16}$$

We are now in a position to define the 'superratio asymmetry', A_{super}, as

$$A_{\mathrm{super}} \;=\; A_{\mathrm{super}}(E_\beta) \;\equiv\; \frac{1-\sqrt{s}}{1+\sqrt{s}}. \tag{F.17}$$

This is explicitly an experimental quantity that is measured directly by the above combination of count rates.

Writing the superratio out explicitly in terms of A' and b', factors of $\varepsilon_{\mathrm{T/B}}$ and $N_{+/-}$ cancel out entirely, and we find that

$$s \;=\; \frac{(1+b'-A')^2}{(1+b'+A')^2}. \tag{F.18}$$

From here it is immediately clear that in absence of other corrections (*e.g.* backscattering, unpolarized background, ...), if $b'=0$ it follows that $A_{\mathrm{super}} = A'$. In the case where $b' \neq 0$, we find that

$$A_{\mathrm{super}} \;=\; \frac{A'}{1+b'} \tag{F.19}$$

$$\approx\; A'\,(1-b'+{b'}^2), \tag{F.20}$$

where we have utilized the assumption that $b' \ll 1$. Thus,

$$A_{\mathrm{super}} \;\approx\; A_\beta\,\frac{v}{c}\,|\vec{P}|\,\langle|\cos\theta|\rangle - A_\beta\,\frac{v}{c}\,|\vec{P}|\,\langle|\cos\theta|\rangle\left(b_{\mathrm{Fierz}}\frac{mc^2}{E_\beta}\right) + A_\beta\,\frac{v}{c}\,|\vec{P}|\,\langle|\cos\theta|\rangle\left(b_{\mathrm{Fierz}}\frac{mc^2}{E_\beta}\right)^2 \tag{F.21}$$

Appendix G

Some Corrections to the Superratio Stuff

We consider further modifications to the rates described in Eqs. (F.2-F.5). In particular, we consider the effect of non-identical polarization magnitudes for the two polarization states and a trap displaced from the center.

We define for the polarization states:

$$P \equiv \frac{1}{2}\left(|\vec{P}_+| + |\vec{P}_+|\right) \tag{G.1}$$

$$\Delta P \equiv \frac{1}{2}\left(|\vec{P}_+| - |\vec{P}_+|\right) \tag{G.2}$$

and immediately find that

$$|\vec{P}_+| = P + \Delta P \tag{G.3}$$

$$|\vec{P}_-| = P - \Delta P. \tag{G.4}$$

Further, we also define:

$$\langle|\cos\theta|\rangle_T \equiv \langle|\cos\theta|\rangle_{\mathrm{T}+} = \langle|\cos\theta|\rangle_{\mathrm{T}-} \tag{G.5}$$

$$\langle|\cos\theta|\rangle_B \equiv \langle|\cos\theta|\rangle_{\mathrm{B}+} = \langle|\cos\theta|\rangle_{\mathrm{B}-}, \tag{G.6}$$

and

$$\langle|\cos\theta|\rangle \equiv \frac{1}{2}\left(\langle|\cos\theta|\rangle_T + \langle|\cos\theta|\rangle_B\right) \tag{G.7}$$

$$\Delta\langle|\cos\theta|\rangle \equiv \frac{1}{2}\left(\langle|\cos\theta|\rangle_T - \langle|\cos\theta|\rangle_B\right). \tag{G.8}$$

It immediately follows that

$$\langle|\cos\theta|\rangle_{\rm T} = \langle|\cos\theta|\rangle + \Delta\langle|\cos\theta|\rangle \tag{G.9}$$

$$\langle|\cos\theta|\rangle_{\rm B} = \langle|\cos\theta|\rangle - \Delta\langle|\cos\theta|\rangle. \tag{G.10}$$

With this new set of variables defined, we can re-write Eqs. (F.2-F.5) as

$$r_{\rm T+}(E_\beta) = \varepsilon_{\rm T}(E_\beta)\, N_+ \left[1 + b' + (A_\beta\frac{v}{c})(P+\Delta P)\left(\langle|\cos\theta|\rangle + \Delta\langle|\cos\theta|\rangle\right)\right] \tag{G.11}$$

$$r_{\rm B+}(E_\beta) = \varepsilon_{\rm B}(E_\beta)\, N_+ \left[1 + b' - (A_\beta\frac{v}{c})(P+\Delta P)\left(\langle|\cos\theta|\rangle - \Delta\langle|\cos\theta|\rangle\right)\right] \tag{G.12}$$

$$r_{\rm T-}(E_\beta) = \varepsilon_{\rm T}(E_\beta)\, N_- \left[1 + b' - (A_\beta\frac{v}{c})(P-\Delta P)\left(\langle|\cos\theta|\rangle + \Delta\langle|\cos\theta|\rangle\right)\right] \tag{G.13}$$

$$r_{\rm B-}(E_\beta) = \varepsilon_{\rm B}(E_\beta)\, N_- \left[1 + b' + (A_\beta\frac{v}{c})(P-\Delta P)\left(\langle|\cos\theta|\rangle - \Delta\langle|\cos\theta|\rangle\right)\right] \tag{G.14}$$

and the superratio becomes

$$s = \frac{\left(1 + b' - (A_\beta\frac{v}{c})(P-\Delta P)\left(\langle|\cos\theta|\rangle + \Delta\langle|\cos\theta|\rangle\right)\right)\left(1 + b' - (A_\beta\frac{v}{c})(P+\Delta P)\left(\langle|\cos\theta|\rangle - \Delta\langle|\cos\theta|\right.}{\left(1 + b' + (A_\beta\frac{v}{c})(P+\Delta P)\left(\langle|\cos\theta|\rangle + \Delta\langle|\cos\theta|\rangle\right)\right)\left(1 + b' + (A_\beta\frac{v}{c})(P-\Delta P)\left(\langle|\cos\theta|\rangle - \Delta\langle|\cos\theta\right.} \tag{G}$$

where $\varepsilon_{\rm T/B}$ and $N_{+/-}$ still completely cancel out. After a bit of algebra, this simplifies to:

$$s = \frac{\left(1 + b' - A' + A_\beta\frac{v}{c}\Delta P\,\Delta\langle|\cos\theta|\rangle\right)^2 - (A_\beta\frac{v}{c})^2\left(\Delta P\langle|\cos\theta|\rangle - P\Delta\langle|\cos\theta|\rangle\right)^2}{\left(1 + b' + A' + A_\beta\frac{v}{c}\Delta P\,\Delta\langle|\cos\theta|\rangle\right)^2 - (A_\beta\frac{v}{c})^2\left(\Delta P\langle|\cos\theta|\rangle + P\Delta\langle|\cos\theta|\rangle\right)^2} \tag{G.16}$$

Note that in the superratio ΔP and $\Delta\langle|\cos\theta|\rangle$ have cancelled out to first order, and the remaining dependencies are quadratic only. Eq. (G.16) is exact, but still a huge enough expression to be pretty unweildy to work with. Let's introduce some

shorthand notation to make this less painful:

$$
\begin{aligned}
A'' &:= A_\beta \frac{v}{c} && \text{(G.17)}\\
c &:= \langle |\cos\theta| \rangle && \text{(G.18)}\\
\Delta c &:= \Delta\langle |\cos\theta| \rangle && \text{(G.19)}\\
r' &:= 1 + b' + A_\beta \frac{v}{c}\, \Delta P\, \Delta\langle |\cos\theta| \rangle && \text{(G.20)}
\end{aligned}
$$

In this notation, we find that

$$
s = \frac{(r'-A')^2 - (A'')^2\,(\Delta P\, c - P\,\Delta c)^2}{(r'+A')^2 - (A'')^2\,(\Delta P\, c + P\,\Delta c)^2}, \qquad \text{(G.21)}
$$

which hurts a lot less to look at. Then, the superratio asymmetry is

$$
\begin{aligned}
A_{\text{super}} &= \frac{1 - \sqrt{\frac{\left(r'-A'\right)^2 - (A'')^2\left(\Delta P\, c - P\,\Delta c\right)^2}{\left(r'+A'\right)^2 - (A'')^2\left(\Delta P\, c + P\,\Delta c\right)^2}}}{1 + \sqrt{\frac{\left(r'-A'\right)^2 - (A'')^2\left(\Delta P\, c - P\,\Delta c\right)^2}{\left(r'+A'\right)^2 - (A'')^2\left(\Delta P\, c + P\,\Delta c\right)^2}}} && \text{(G.22)}\\
&= \frac{\left[\sqrt{(r'+A')^2 - (A'')^2\,(\Delta P\, c + P\,\Delta c)^2} - \sqrt{(r'-A')^2 - (A'')^2\,(\Delta P\, c - P\,\Delta c)^2}\right]^2}{\left[(r'+A')^2 - (A'')^2\,(\Delta P\, c + P\,\Delta c)^2\right] - \left[(r'-A')^2 - (A'')^2\,(\Delta P\, c - P\,\Delta c)^2\right]} && \text{(G.23)}\\
&= \frac{\begin{pmatrix} 2\left[(r')^2 + (A')^2 - (A'')^2\left((P\,\Delta c)^2 + (\Delta P\, c)^2\right)\right] \\ -2\left[(r'+A')^2 - (A'')^2\,(\Delta P\, c + P\,\Delta c)^2\right]^{1/2}\left[(r'-A')^2 - (A'')^2\,(\Delta P\, c - P\,\Delta c)^2\right]^{1/2} \end{pmatrix}}{4\left[(r'\,A') - (A'')^2\,(P\, c\,\Delta P\,\Delta c)\right]} && \text{(G.24)}
\end{aligned}
$$

Appendix H

Constraining the Analysis with Lifetime Measurements

H.1 Background/Introduction

The goal here is to understand what physical interpretation to give to (linear combinations of) G4 simulations with sets of coupling constants that may or may not be physically possible, given previous lifetime measurements that were not taken into account. The results aren't broken forever or anything, but some care must be given to the interpretation.

We'll loosely follow Severijns et. al.'s procedure [**?**]. In this paper, (which conveniently sets b_{Fierz} to zero as soon as the math starts getting messy), we see that the authors will eventually need to split their treatment into "Fermi" and "Gamow-Teller" parts to arrive at their final result. This becomes clear upon examining their 1D decay rate element:

$$d\Gamma \;=\; (\text{constants})\;\xi\left(1+\frac{m}{W}b\right)F(\pm Z,W)S(\pm Z,W)(W-W_0)^2pW\,dW \quad \text{(H.1)}$$

where we find that the nuclear shape correction function, $S(\pm Z,W)$, is slightly different in the case of Fermi and Gamow-Teller decays. Though they note that $S(\pm Z,W)=1$ for both types of decay under the allowed approximation, and it changes only slightly under a more complete treatment, it is this term which gives rise to the statistical rate functions f_V and f_A. Note that the overall value of the

ratio f_A/f_V directly changes any estimate of the mixing ratio ρ, so we will need at least an estimate of its value in order to do anything useful.

In particular,

$$f_{V/A} \;=\; \int F(\pm Z, W) S_{V/A}(\pm Z, W)(W - W_0)^2 pW \, dW \tag{H.2}$$

No matter the form of $S(\pm Z, W)$ — and I definitely *do not* know its form — this is clearly a very challenging integral. Luckily, a calculation result is provided (with no associated uncertainty given):

$$\left.\frac{f_A}{f_V}\right|_{37K} = 1.00456. \tag{H.3}$$

So, we follow their calculation through, and at the end it yields this result:

$$Ft^{\text{mirror}} \;=\; \frac{2Ft^{0^+\to 0^+}}{1 + \frac{f_A}{f_V}\rho^2}, \tag{H.4}$$

with

$$\rho \approx \frac{C_A M^0_{GT}}{C_V M^0_F}. \tag{H.5}$$

But of course, there's no reason why we can't do a similar calculation while including non-zero values of C_S and C_T. Probably.

H.2 Now What?

In the case where $b_{\text{Fierz}} = 0$, this treatment gets us to the sort of results we might want. However, if we start introducing non-zero scalar or tensor coupling constants, it's unclear (to me) how we should treat the associated shape correction function(s). Eg, do we think the shape correction function $S_V(\pm Z, W)$ is associated with a *Fermi* decay, or with a *vector* coupling? In the case of zero scalar or tensor couplings, the question is irrelevant because the calculation must be the same either way – M_F and C_V go together every time.

With $b_{\text{Fierz}} \neq 0$, the distinction changes the calculation though, since its terms have factors of (eg) $M_F^2 C_V$. Perhaps there are a whole different set of shape correction

functions associated specifically with C_S and C_T.

I *might* be able to find a treatment in the literature somewhere where they do one thing or the other. For my own mental clarity, I would really like to know the answer. However, I recognize that for the purpose of evaluating scalar and tensor coupling constants, the distinction is largely academic, and won't really affect the answer. I have to just pick something and go with it.

H.3 After Picking Something...

I declare (and so it has to be true, regardless of reality) that the shape correction function $S_{V/A}(\pm Z, W)$ is associated with the matrix element $M_{F/GT}$ rather than the coupling constant $C_{V/A}$. So, given this, we'll switch our notation a bit and write down a new decay rate:

$$d\Gamma = \left(\vec{\xi} + \frac{m}{W}\,(\vec{b\xi})\right) \cdot d\vec{\Gamma}_0, \tag{H.6}$$

where the vector components are the Fermi and Gamow-Teller components of the decay:

$$\vec{\xi} = \begin{bmatrix} 2M_F^2\ (C_V^2 + C_S^2) \\ 2M_{GT}^2 (C_A^2 + C_T^2) \end{bmatrix} \tag{H.7}$$

$$(\vec{b\xi}) = \begin{bmatrix} \pm 2\gamma\, \mathrm{Re}[C_S C_V^* + C_S' C_V'^*] \\ \pm 2\gamma\, \mathrm{Re}[C_T C_A^* + C_T' C_A'^*] \end{bmatrix} \tag{H.8}$$

$$d\vec{\Gamma}_0 = (\text{constants}) \begin{bmatrix} F_F(\pm Z, W)\ S_F(\pm Z, W)\ (W - W_0)^2\, pW\, dW \\ F_{GT}(\pm Z, W) S_{GT}(\pm Z, W) (W - W_0)^2\, pW\, dW \end{bmatrix}. \tag{H.9}$$

We find that the integrals involved here are still hard. I will need to make some simplifying assumptions to get anywhere.

Appendix I

A PDF For The People

I.1 JTW

Here's an equation!

$$\begin{aligned}\omega(\cdots)\mathrm{d}E_\beta\,\mathrm{d}^3\hat{\boldsymbol{\Omega}}_{\boldsymbol{\beta}}\,\mathrm{d}^3\hat{\boldsymbol{\Omega}}_{\boldsymbol{\nu}} &= \frac{F_+(Z,E_\beta)}{(2\pi)^5}\,p_\beta E_\beta(E_0-E_\beta)^2\mathrm{E}_\beta\,\mathrm{d}^3\hat{\boldsymbol{\Omega}}_{\boldsymbol{\beta}}\,\mathrm{d}^3\hat{\boldsymbol{\Omega}}_{\boldsymbol{\nu}}\,\xi\left\{1+a_{\beta\nu}\frac{\vec{\boldsymbol{p}}_{\boldsymbol{\beta}}\cdot\vec{\boldsymbol{p}}_{\boldsymbol{\nu}}}{E_\beta E_\nu}+b_{\mathrm{Fierz}}\frac{m_e c^2}{E_\beta}\right.\\ &\quad +c_{\mathrm{align}}\left(\frac{\vec{\boldsymbol{p}}_{\boldsymbol{\beta}}\cdot\vec{\boldsymbol{p}}_{\boldsymbol{\nu}}}{3E_\beta E_\nu}-\frac{(\vec{\boldsymbol{p}}_{\boldsymbol{\beta}}\cdot\hat{\boldsymbol{j}})(\vec{\boldsymbol{p}}_{\boldsymbol{\nu}}\cdot\hat{\boldsymbol{j}})}{E_\beta E_\nu}\right)\left(\frac{J(J+1)-3\langle(\vec{\boldsymbol{J}}\cdot\hat{\boldsymbol{j}})^2\rangle}{J(2J-1)}\right)\\ &\quad \left.+\frac{\vec{\boldsymbol{J}}}{J}\cdot\left(A_\beta\frac{p_\beta}{E_\beta}+B_\nu\frac{p_\nu}{E_\nu}+D_{\mathrm{TR}}\frac{\vec{\boldsymbol{p}}_{\boldsymbol{\beta}}\times\vec{\boldsymbol{p}}_{\boldsymbol{\nu}}}{E_\beta E_\nu}\right)\right\}\end{aligned} \tag{I.1}$$

We haven't integrated out the neutrino momentum. Neutrino energy itself is a redundant parameter, I think, because we are already using an endpoint energy and a beta energy, and we are not taking recoil-order effects into account.

For "convenience", let's define a nuclear alignment term, T_{align}, so that:

$$T_{\mathrm{align}} = \frac{J(J+1)-3\langle(\vec{\boldsymbol{J}}\cdot\hat{\boldsymbol{j}})^2\rangle}{J(2J-1)} \tag{I.2}$$

I.2 Holstein

This one is harder. But here, we've already integrated over neutrino momentum at least. That's something. Here's Holstein's Eq. (52):

$$
\begin{aligned}
\mathrm{d}^3\Gamma &= 2G_v^2 \cos^2\theta_c \frac{F_+(Z,E_\beta)}{(2\pi)^4} p_\beta E_\beta (E_0 - E_\beta)^2 \mathrm{E}_\beta \, \mathrm{d}^3\hat{\boldsymbol{\Omega}}_{\boldsymbol{\beta}} \\
&\times \left\{ F_0(E_\beta) + \Lambda_1 F_1(E_\beta) \hat{\boldsymbol{n}} \cdot \frac{\vec{\boldsymbol{p}}_{\boldsymbol{\beta}}}{E_\beta} + \Lambda_2 F_2(E_\beta) \left[\left(\hat{\boldsymbol{n}} \cdot \frac{\vec{\boldsymbol{p}}_{\boldsymbol{\beta}}}{E_\beta} \right)^2 - \frac{1}{3} \frac{p_\beta^2}{E_\beta^2} \right] \right. \\
&\left. + \Lambda_3 F_3(E_\beta) \left[\left(\hat{\boldsymbol{n}} \cdot \frac{\vec{\boldsymbol{p}}_{\boldsymbol{\beta}}}{E_\beta} \right)^3 - \frac{3}{5} \frac{p_\beta^2}{E_\beta^2} \hat{\boldsymbol{n}} \cdot \frac{\vec{\boldsymbol{p}}_{\boldsymbol{\beta}}}{E_\beta} \right] \right\} \qquad \text{(I.3)}
\end{aligned}
$$

Let's define some of that notation! Firstly,

$$
\hat{\boldsymbol{n}} = \hat{\boldsymbol{j}}, \qquad \text{(I.4)}
$$

and the Λ_i are given by Holstein's Eq. (48):

$$
\Lambda_1 := \frac{\langle M \rangle}{J} \qquad \text{(I.5)}
$$

$$
\Lambda_2 := 1 - \frac{3\langle M^2 \rangle}{J(J+1)} \qquad \text{(I.6)}
$$

$$
\Lambda_3 := \frac{\langle M \rangle}{J} - \frac{5\langle M^3 \rangle}{J(3J^2+3J-1)}. \qquad \text{(I.7)}
$$

We immediately see that Holstein's Λ_1 is closely related to JTW's $\frac{\vec{\boldsymbol{J}}}{J}$, and a bit later after John points it out to us, we see that Holstein's Λ_2 is closely related to JTW's T_{align}. JTW doesn't have any equivalent to Λ_3. In particular, we find:

$$
\Lambda_1 \hat{\boldsymbol{j}} = \frac{\langle M \rangle}{J} \hat{\boldsymbol{j}} = \frac{\vec{\boldsymbol{J}}}{J} \qquad \text{(I.8)}
$$

$$
\Lambda_2 = T_{\mathrm{align}} \frac{(2J-1)}{(J+1)}. \qquad \text{(I.9)}
$$

Now we'll have to deal with expanding the $F_i(E_\beta)$. Holstein makes a goddamn mess of this, so here we go! From Holstein's Eq. (B10):

$$
F_i(E_\beta) = H_i(E_\beta, J, J', 0). \qquad \text{(I.10)}
$$

From Holstein's many Eqs. (B7), we see that the $H_i(E_\beta, u, v, s)$ can be written in terms of the functions $F_i(E_\beta, u, v, s)$, which we carefully note *are not the same* as

the functions $F_i(E_\beta)$. We further see, from Holstein's Eq. (B9) that a further set of functions, $f_i(E_\beta)$ are defined in terms of the $F_i(E_\beta, u, v, s)$. In particular, Holstein's Eq. (B9) states that

$$f_i(E_\beta) \;=\; F_i(E_\beta, J, J', 0). \tag{I.11}$$

Then, if we combine (some parts of) Holstein's Eqs. (B7) with (B9) and (B10)

$$F_0(E_\beta) \;=\; H_0(E_\beta, J, J', 0) \;=\; F_1(E_\beta, J, J', 0) \;=\; f_1(E_\beta) \tag{I.12}$$

$$F_1(E_\beta) \;=\; H_1(E_\beta, J, J', 0) \;=\; F_4(E_\beta, J, J', 0) + \frac{1}{3}F_7(E_\beta, J, J', 0) \;=\; f_4(E_\beta) + \frac{1}{3}f_7(E_\beta) \tag{I.13}$$

$$F_2(E_\beta) \;=\; H_2(E_\beta, J, J', 0) \;=\; F_{10}(E_\beta, J, J', 0) + \frac{1}{2}F_{13}(E_\beta, J, J', 0) \;=\; f_{10}(E_\beta) + \frac{1}{3}f_{13}(E_\beta) \tag{I.14}$$

$$F_3(E_\beta) \;=\; H_3(E_\beta, J, J', 0) \;=\; F_{18}(E_\beta, J, J', 0) \;=\; f_{18}(E_\beta). \tag{I.15}$$

So that's fun. Note that the $f_i(E_\beta)$ are what goes into the polarized decay spectrum when the neutrino (ie, the recoil) is also observed. It's a more complicated spectrum that way. For this spectrum in which the neutrino has already been integrated over, we can just look up the $H_i(E_\beta, J, J', 0) = H_i(E_\beta, u, v, s)$ spectral functions, and leave it at that.

So let's do this thing!

$$\begin{aligned} F_0(E_\beta) &= |a_1|^2 + 2Re\left[a_1^* a_2\right]\frac{1}{3M^2}\left[m_e^2 + 4E_\beta E_0 + 2\frac{m_e^2}{E_\beta}E_0 - 4E_\beta^2\right] \\ &+|c_1|^2+2Re\left[c_1^* c_2\right]\frac{1}{9M^2}\left[11m_e^2 + 20E_\beta E_0 - 2\frac{m_e^2}{E_\beta}E_0 - 20E_\beta^2\right] - 2\frac{E_0}{3M}Re\left[c_1^*(c_1 + d \pm b)\right] \\ &+\frac{2E_\beta}{3M}\left(3\left|a_1\right|^2 + Re\left[c_1^*(5c_1 \pm 2b)\right]\right) - \frac{m_e^2}{3ME_\beta}Re\left[-3a_1^* e + c_1^*\left(2c_1 + d \pm 2b - h\frac{E_0 - E_\beta}{2M}\right)\right] \end{aligned} \tag{I.16}$$

$$F_1(E_\beta) = \delta_{u,v}\left(\frac{u}{u+1}\right)^{1/2}\Bigg\{2Re\left[a_1^*\left(c_1 - \frac{E_0}{3M}(c_1+d\pm b) + \frac{E_\beta}{3M}(7c_1 \pm b + d)\right)\right]$$
$$+2Re\left[a_1^* c_2 + c_1^* a_2\right]\left(\frac{4E_\beta(E_0-E_\beta)+3m_e^2}{3M^2}\right)\Bigg\}$$
$$\mp\frac{(-1)^s\gamma_{u,v}}{u+1}Re\left[c_1^*\left(c_1 + 2c_2\left(\frac{8E_\beta(E_0-E_\beta)+3m_e^2}{3M^2}\right) - \frac{2E_0}{3M}(c_1+d\pm b) + \frac{E_\beta}{3M}(11c_1 - d \pm 5b)\right)\right]$$
$$+\frac{\lambda_{u,v}}{u+1}Re\left[c_1^*\left(-f\left(\frac{5E_\beta}{M}\right) + g\left(\frac{3}{2}\right)^{1/2}\left(\frac{E_0^2 - 11E_0E_\beta + 6m_e^2 + 4E_\beta^2}{6M^2}\right) \pm 3j_2\left(\frac{8E_\beta^2 - 5E_0E_\beta - 3m_e^2}{6M^2}\right)\right)\right] \tag{I.17}$$

$$F_2(E_\beta) = \theta_{u,v}\frac{E_\beta}{2M}Re\left[c_1^*\left(c_1 + c_2\frac{8(E_0-E_\beta)}{3M} - d \pm b\right)\right]$$
$$-\delta_{u,v}\frac{E_\beta}{M}\left[\frac{u(u+1)}{(2u-1)(2u+3)}\right]^{1/2}Re\left[a_1^*\left(\left(\frac{3}{2}\right)^{1/2}f + g\frac{E_\beta+2E_0}{4M} \pm \left(\frac{3}{2}\right)^{1/2}j_2\frac{E_0-E_\beta}{2M}\right)\right]$$
$$+(-1)^s\kappa_{u,v}\frac{E_\beta}{2M}Re\left[c_1^*\left(\pm 3f \pm \left(\frac{3}{2}\right)^{1/2}g\frac{E_0-E_\beta}{M} + 3j_2\frac{E_0-2E_\beta}{2M}\right)\right] + \epsilon_{u,v}Re\left[c_1^* j_3\right]\left(\frac{21E_\beta^2}{8M^2}\right) \tag{I.18}$$

$$F_3(E_\beta) = -\delta_{u,v}(3u^2+3u-1)\left[\frac{u}{(u-1)(u+1)(u+2)(2u-1)(2u+3)}\right]^{1/2}Re\left[a_1^* j_3\right]\left(\frac{E_\beta^2\sqrt{15}}{4M^2}\right)$$
$$+\frac{\rho_{u,v}}{u+1}Re\left[c_1^*(g\sqrt{3} + j_2\sqrt{2})\left(\frac{5E_\beta^2}{4M^2}\right)\right] \pm \frac{(-1)^s\sigma_{u,v}}{u+1}Re\left[c_1^* j_3\right]\left(\frac{5E_\beta^2}{2M^2}\right) \tag{I.19}$$

...Phew! I typed all of that out just so that I can have a record of what's going on here, but actually, the very first thing I want to do is make some simplifications here. If we evaluate Holstein's Eqs. (B8), which I will absolutely not type out here, for the

case $u = v = J = J' = 3/2$, we find the following values:

$$\begin{aligned}
\delta_{u,v} &= 1 & \theta_{u,v} &= 1 & \rho_{u,v} &= \frac{-41}{40} \\
\gamma_{u,v} &= 1 & \kappa_{u,v} &= \frac{1}{2\sqrt{2}} & \sigma_{u,v} &= \frac{-41}{4\sqrt{35}} \\
\lambda_{u,v} &= \frac{-\sqrt{2}}{5} & \epsilon_{u,v} &= \frac{-1}{2\sqrt{5}} & \phi_{u,v} &= 0
\end{aligned} \tag{I.20}$$

Furthermore, in our calculations here, we will be considering only the β^+ decay modes, and therefore we take the *lower* sign when the option arises. We also will use $s = 0$, so that $(-1)^s = +1$.

Appendix J

Holstein/JTW Comparison Confusion

Ben at pg 17(30) claims the relation between JTW and Holstein for A_β is:

$$A_\beta = \frac{f_4(E) + \frac{1}{3} f_7(E)}{f_1(E)} \tag{J.1}$$

See, it's counterintuitive, because I would have guessed that it would be just

$$A_\beta = \frac{f_4(E)}{f_1(E)} \tag{J.2}$$

...But it's not. That extra f_7 term is there, being weird. In Holstein (51), it's all like,

$$d^5\Gamma = (...) + (...) * \Lambda_1(\hat{n} \cdot \hat{k})(\frac{\vec{p}}{E} \cdot \hat{k})\, f_7(E), \tag{J.3}$$

and that just doesn't look like A_β.

So, maybe there's some magic that happens when you integrate it and it turns into (52). From (52), I would (naively??) think that:

$$A_\beta = \frac{F_1(E)}{F_0(E)} \tag{J.4}$$

Is it even true?!? Let's see what Holstein has to say...

In general,

$$f_i(E) = F_i(E, J, J', 0) \tag{J.5}$$
$$F_i(E) = H_i(E, J, J', 0) \tag{J.6}$$

So here specifically, we have:

$$F_0(E) = H_0(E, u, v, s) = F_1(E, u, v, s) \tag{J.7}$$
$$F_1(E) = H_1(E, u, v, s) = F_4(E, u, v, s) + \frac{1}{3}F_7(E, u, v, s) \tag{J.8}$$
$$= f_4(E) + \frac{1}{3}f_7(E) \tag{J.9}$$

So I guess whatever the fuck Ben did to get his result checks out, and my naive supposition was correct. But now how do I translate that into JTW for anything else?!

JTW just straight-up has *nothing* that corresponds to the f_7 term in Holstein. The integral that puts f_7 into A_β has simply *not been done* at the point where JTW writes down their equation.

So, okay, let's take a look at how the dominant terms in f_4, f_1, and f_7 scale. From Holstein (pg 807):

$$f_1(E) \approx a_1^2 + c_1^2 \tag{J.10}$$
$$f_4(E) \approx (\text{const}) * 2a_1c_1 + (\text{const})c_1^2 \tag{J.11}$$
$$f_7(E) \approx (\text{const}) * a_1c_1\frac{E0}{M} + (\text{const})a_1c_1\frac{E}{M} + (\text{const})c_1^2\frac{E0}{2M} + (\text{const})c_1^2\frac{E}{2M} \tag{J.12}$$

OK, so I think f_7 wouldn't be included in JTW anyway, because it's too high order in E/M. (Is there really nothing in f_7 that's not multiplied by at least one factor of $1/M$?? .... yep, nothing.)

So here's what Coulomb-JTW says (set $C_S = C'_S = C_T = C'_T = 0$, and require that $C_A = C'_A$ and $C_V = C'_V$ are real):

$$\xi = |M_F|^2(2C_V^2) + |M_{GT}|^2(2C_A^2) \quad \text{(J.13)}$$

$$A_\beta\xi = |M_{GT}|^2\frac{1}{J+1}\left[+2C_A^2 + M_F M_{GT}\left(\frac{J}{J+1}\right)^{1/2} * (-2C_V C_A)\right] \quad \text{(J.14)}$$

Indeed, there are no E/M terms. So we agree with ourselves here. That's nice. But actually, we need to figure out how to convert *all* of the JTW letters into Holstein notation. Not just A_β. Of particular importance is anything with a *linear* dependence on C_T (or C_S). That includes $bFierz$, for which there is no Holstein equivalent, but also:

- Real parts of $b_{\rm Fierz}$
- Imaginary parts of $a_{\beta\nu}$
- Imaginary parts of $c_{\rm align}$
- Imaginary parts of A_β
- Real parts of B_ν
- Real parts of $D_{\rm TR}$

...which is actually all of the things. All of them. So, I claim these are the relationships:

$$\xi = f_1(E) \qquad (?) \quad \text{(J.15)}$$

$$a_{\beta\nu} = f_2(E) \,/\, f_1(E) \quad \text{(J.16)}$$

$$\frac{\langle\vec{J}\rangle}{J}\cdot\frac{\vec{p}}{E}\,A_\beta = \Lambda_1\hat{n}\cdot\frac{\vec{p}}{E}\,f_4(E) \,/\, f_1(E) \quad \text{(J.17)}$$

$$\frac{\langle\vec{J}\rangle}{J}\cdot\frac{\vec{p}_\nu}{E_\nu}B_\nu = \Lambda_1\hat{n}\cdot\vec{k}\;\; f_6(E) \,/\, f_1(E) \quad \text{(J.18)}$$

$$\frac{\langle\vec{J}\rangle}{J}\cdot\frac{(\vec{p}\times\vec{p}_\nu)}{EE_\nu}D_{\rm TR} = \Lambda_1\hat{n}\cdot(\frac{\vec{p}}{E}\times\hat{k}\,)\;\; f_8(E) \,/\, f_1(E) \quad \text{(J.19)}$$

$$\left[\frac{J(J+1)-3\langle(\vec{J}\cdot\hat{j})^2\rangle}{J(2J-1)}\right]\left[\frac{1}{3}\frac{\vec{p}\cdot\vec{p}_\nu}{EE_\nu} - \frac{(\vec{p}\cdot\hat{j})(\vec{p}_\nu\cdot\hat{j})}{EE_\nu}\right]c_{\rm align} = \Lambda_2\left[(\hat{n}\cdot\frac{\vec{p}}{E})(\hat{n}\cdot\hat{k}) - \frac{1}{3}(\frac{\vec{p}}{E}\cdot\hat{k}\,)\right]\;\; f_{12}(E) \,/\, f_1(E) \quad \text{(J.20)}$$

Other Holstein terms in (51) have no JTW equivalent, either because JTW didn't include recoil-order corrections, or because JTW didn't bother with higher multipole moments. These Holstein-specific spectral functions are not used in JTW:

- $f_3(E)$ (dipole)
- $f_5(E)$ (dipole)
- $f_7(E)$ (dipole)
- $f_9(E)$ (dipole)
- $f_{10}(E)$ (quadrupole)
- $f_{11}(E)$ (quadrupole)
- $f_{13}(E)$ (quadrupole)
- $f_1(E)$ (quadrupole, used elsewhere)
- $f_{16}(E)$ (quadrupole)
- $f_{17}(E)$ (quadrupole)
- Octopoles: f_{18}, f_{19}, f_{20}, f_{21}, f_{22}, f_{23}, f_{24}
- 16-poles: f_{25}, f_{26}, f_{27}.

OK, so what needs to happen now is for me to convert the JTW alphabet into *other* Holstein notation. Since I know how they scale with the $f_i(E)$'s, let's see if we can convert those specific $f_i(E)$'s into any of the Holstein notation that is going into my code – ie, the $F_i(E)$'s. In particular, we'll want $f_1(E)$, $f_2(E)$, $f_4(E)$, $f_6(E)$, $f_8(E)$, $f_12(E)$. This will actually have the pleasant side-effect of telling us how to fucking do that goddamn neutrino momentum integral in JTW. I think. So, from Holstein:

- $f_1(E) \;=\; F_1\,(E,u,v,s) \;=\; H_0(E,u,v,s) = F_0(E)$
- $f_2(E) \;=\; F_2\,(E,u,v,s) \;= ?$
- $f_4(E) \;=\; F_4\,(E,u,v,s) \;= ?$

- $f_6(E) \;=\; F_6\,(E,u,v,s) \;= ?$
- $f_8(E) \;=\; F_8\,(E,u,v,s) \;= ?$
- $f_{12}(E) = \; F_{12}(E,u,v,s) \;= ?$

...which, let's be honest, doesn't really help. Let's go the other direction, then.

- $F_0(E) = H_0(E,u,v,s) = F_1(E,u,v,s) = f_1(E)$ as before, but also:
- $F_1(E) = H_1(E,u,v,s) = F_4(E,u,v,s) + \frac{1}{3}F_7(E,u,v,s) = f_4(E) + \frac{1}{3}f_7(E)$
- $F_2(E) = H_2(E,u,v,s) = F_{10}(E,u,v,s) + \frac{1}{3}F_{13}(E,u,v,s) = f_{10}(E) + \frac{1}{3}f_{13}(E)$
- $F_3(E) = H_3(E,u,v,s) = F_{18}(E,u,v,s) = f_{18}(E)$

So, okay, I can write *my* PDF in terms of only Holstein's $f_1(E)$, $f_4(E)$, $f_7(E)$, $f_{10}(E)$, $f_{13}(E)$, $f_{18}(E)$. I can write JTW's PDF in terms of only Holstein's $f_1(E)$, $f_2(E)$, $f_4(E)$, $f_6(E)$, $f_8(E)$, $f_{12}(E)$. Those ... aren't the same thing. Like, at all. If I integrate those, do they come out to be the same things? Somehow?

OK. I can separate some terms out into what they *should* correspond to based on their multipole dependence... Roughly speaking,

$$F_0(E) \;\leftrightarrow\; f_1(E) \quad \text{(obviously)} \tag{J.21}$$
$$F_1(E) \;\leftrightarrow\; f_4(E),\; f_5(E),\; f_6(E),\; f_7(E),\; f_8(E),\; f_9(E) \tag{J.22}$$
$$F_2(E) \;\leftrightarrow\; f_{10}(E),\; f_{11}(E),\; f_{12}(E),\; f_{13}(E),\; f_1(E),\; f_{16}(E) \tag{J.23}$$
$$F_3(E) \;\leftrightarrow\; \text{...who even cares?} \tag{J.24}$$

- * Check: in Holstein, are there simple relationships between those things?
- * Check: if I do the integrals of the momentum-thingies multiplying those specific $f_i(E)$'s in Eq. (51) do they turn out the way I expect? ie, do I recover the corresponding terms in Eq. (52)?

Appendix K

Compare by Multipoles!

My code uses Holstein's Eq. (52), rather than Eq. (51). In his notation, I'm using $F_i(E)$'s rather than $f_i(E)$'s. I need to convert between them. This is because:

- (a): Coulomb/Radiative corrections (some terms, up to $f_1 5(E)$):
  f_1, f_2, f_4, f_6, f_7, $f_1 2$, $f_1 4$, $f_1 5$
- (b): C_S/C_T inclusion (JTW has equivalents for only some terms, up to $f_1 2(E)$):
  f_1, f_2, f_4, f_6, f_8, $f_1 2$.

Holstein and JTW terms have *this* relationship:

$$
\begin{aligned}
\xi &= f_1(E) && \text{(? times some constant? do} \\
a_{\beta\nu} &= f_2(E) \,/\, f_1(E) \\
\frac{\langle \vec{J} \rangle}{J} \cdot \frac{\vec{p}}{E}\, A_\beta &= \Lambda_1 \hat{n} \cdot \frac{\vec{p}}{E}\, f_4(E) \,/\, f_1(E) \\
\frac{\langle \vec{J} \rangle}{J} \cdot \frac{\vec{p}_\nu}{E_\nu} B_\nu &= \Lambda_1 \hat{n} \cdot \vec{k}\ \ f_6(E) \,/\, f_1(E) \\
\frac{\langle \vec{J} \rangle}{J} \cdot \frac{(\vec{p} \times \vec{p}_\nu)}{E E_\nu} D_{\rm TR} &= \Lambda_1 \hat{n} \cdot (\frac{\vec{p}}{E} \times \hat{k}\,)\ \ f_8(E) \,/\, f_1(E) \\
\left[\frac{J(J+1) - 3\langle (\vec{J}\cdot\hat{j})^2 \rangle}{J(2J-1)} \right] \left[\frac{1}{3} \frac{\vec{p}\cdot\vec{p}_\nu}{E E_\nu} - \frac{(\vec{p}\cdot\hat{j})(\vec{p}_\nu\cdot\hat{j})}{E E_\nu} \right] c_{\rm align} &= \Lambda_2 \left[(\hat{n}\cdot\frac{\vec{p}}{E})(\hat{n}\cdot\hat{k}) - \frac{1}{3}(\frac{\vec{p}}{E}\cdot\hat{k}\,) \right]\ \ f_{12}(E) \,/\, f_1(E)
\end{aligned}
$$

- JTW Monopole Terms: $\xi, \quad \xi \frac{m}{E} * b_{\rm Fierz}, \quad \xi \frac{\vec{p}\cdot\vec{p}_\nu}{E E_\nu} * a_{\beta\nu}$
- JTW Dipole Terms: $\xi \frac{\langle \vec{J} \rangle}{J} \cdot \frac{\vec{p}}{E} * A_\beta, \quad \xi \frac{\langle \vec{J} \rangle}{J} \cdot \frac{\vec{p}_\nu}{E_\nu} * B_\nu, \quad \xi \frac{\langle \vec{J} \rangle}{J} \cdot \frac{\vec{p} \times \vec{p}_\nu}{E E_\nu} * D_{\rm TR}$

- JTW Quadrupole Terms: $\xi\left(\frac{J(J+1)-3\langle(\vec{J}\cdot\hat{j})^2\rangle}{J(2J-1)}\right)\left(\frac{1}{3}\frac{\vec{p}\cdot\vec{p}_\nu}{EE_\nu}-\frac{(\vec{p}\cdot\hat{j})(\vec{p}_\nu\cdot\hat{j})}{EE_\nu}\right)*c_{\text{align}}$

...

- Holstein (52) Monopole Term:
  $F_0(E)=f_1(E)$

- Holstein (52) Dipole Term:
  $\Lambda_1\,(\hat{n}\cdot\frac{\vec{p}}{E})\;*\;F_1(E)$
  $=\Lambda_1\,(\hat{n}\cdot\frac{\vec{p}}{E})*\big(\,f_4(E)+\frac{1}{3}f_7(E)\big)$

- Holstein (52) Quadrupole Term:
  $\Lambda_2\left((\hat{n}\cdot\frac{\vec{p}}{E})^2-\frac{1}{3}\frac{p^2}{E^2}\right)*F_2(E)$
  $=\Lambda_2\left((\hat{n}\cdot\frac{\vec{p}}{E})^2-\frac{1}{3}\frac{p^2}{E^2}\right)*\big(\,f_{10}(E)+\frac{1}{3}f_{13}(E)\big)$
  $=\Lambda_2T_2(\hat{n}):[\frac{\vec{p}}{E},\frac{\vec{p}}{E}]*\big(\,f_{10}(E)+\frac{1}{3}f_{13}(E)\big)$

- Holstein (52) Octopole Term:
  $\Lambda_3\left((\hat{n}\cdot\frac{\vec{p}}{E})^3-\frac{3}{5}\frac{p^2}{E^2}(\hat{n}\cdot\frac{\vec{p}}{E})\right)*F_3(E)$
  $=\Lambda_3\left((\hat{n}\cdot\frac{\vec{p}}{E})^3-\frac{3}{5}\frac{p^2}{E^2}(\hat{n}\cdot\frac{\vec{p}}{E})\right)*\;f_{18}(E)$
  $=\Lambda_3T_3(\hat{n}):[\frac{\vec{p}}{E},\frac{\vec{p}}{E},\frac{\vec{p}}{E}]*\;f_{18}(E)$

- Holstein (52) Hexadecapole Term:
  (none)

...

- Holstein (51) Monopole Terms:
  $f_1(E),\qquad\frac{\vec{p}\cdot\hat{k}}{E}*f_2(E),\qquad\left(\frac{(\vec{p}\cdot\hat{k})^2}{E^2}-\frac{1}{3}\frac{p^2}{E^2}\right)*f_3(E)$

- Holstein (51) Dipole Terms:
  $\Lambda_1\,(\hat{n}\cdot\frac{\vec{p}}{E})*f_4(E),\qquad\Lambda_1\,(\hat{n}\cdot\frac{\vec{p}}{E})\frac{\vec{p}\cdot\hat{k}}{E}*\;f_5(E),$
  $\Lambda_1(\hat{n}\cdot\hat{k})*f_6(E),\qquad\Lambda_1(\hat{n}\cdot\hat{k})\frac{\vec{p}\cdot\hat{k}}{E}*f_7(E),$
  $\Lambda_1\hat{n}\cdot\left(\frac{\vec{p}}{E}\times\hat{k}\right)*f_8(E)\qquad\Lambda_1\hat{n}\cdot\left(\frac{\vec{p}}{E}\times\hat{k}\right)\frac{\vec{p}\cdot\hat{k}}{E}*f_9(E)$

- Holstein (51) Quadrupole Terms:
  $\Lambda_2T_2(\hat{n}):[\frac{\vec{p}}{E},\frac{\vec{p}}{E}]*f_{10}(E),\qquad\Lambda_2T_2(\hat{n}):[\frac{\vec{p}}{E},\frac{\vec{p}}{E}]\,(\frac{\vec{p}\cdot\hat{k}}{E})*f_{11}(E),$

$\Lambda_2 T_2(\hat{n}) : [\frac{\vec{p}}{E}, \hat{k}] * f_{12}(E), \qquad \Lambda_2 T_2(\hat{n}) : [\frac{\vec{p}}{E}, \hat{k}]\,(\frac{\vec{p}\cdot\hat{k}}{E}) * f_{13}(E),$

$\Lambda_2 T_2(\hat{n}) : [\hat{k}, \hat{k}] * f_{14}(E), \qquad \Lambda_2 T_2(\hat{n}) : [\hat{k}, \hat{k}]\,(\frac{\vec{p}\cdot\hat{k}}{E}) * f_{15}(E) \quad (?)$

$\Lambda_2 T_2(\hat{n}) : [\frac{\vec{p}}{E}, \frac{\vec{p}}{E} \times \hat{k}] * f_{16}(E),$

$\Lambda_2 T_2(\hat{n}) : [\hat{k}, \frac{\vec{p}}{E} \times \hat{k}] * f_{17}(E)$

- Holstein (51) Octopole Terms:
  $\Lambda_3 T_3(\hat{n}) : [\frac{\vec{p}}{E}, \frac{\vec{p}}{E}, \frac{\vec{p}}{E}] * f_{18}(E)$
  (also some other stuff, but this is the only term that doesn't integrate to zero.)

- Holstein (51) Hexadecapole Terms:
  (some stuff. don't care.)

Holstein's tensor notation definitions:

$$T_2(\hat{n}) : [\vec{a}, \vec{b}] = \left((\hat{n}\cdot\vec{a})(\hat{n}\cdot\vec{b}) - \frac{1}{3}\vec{a}\cdot\vec{b} \right) \tag{K.7}$$

$$T_3(\hat{n}) : [\vec{a}, \vec{b}, \vec{c}] = \left((\hat{n}\cdot\vec{a})(\hat{n}\cdot\vec{b})(\hat{n}\cdot\vec{c}) - \frac{1}{5}\left((\hat{n}\cdot\vec{a})(\vec{b}\cdot\vec{c}) + (\hat{n}\cdot\vec{b})(\vec{a}\cdot\vec{c}) + (\hat{n}\cdot\vec{c})(\vec{a}\cdot\vec{b}) \right) \right) \tag{K.8}$$

$$T_4(\hat{n}) : [\vec{a}, \vec{b}, \vec{c}, \vec{d}] = \text{(some stuff)} \tag{K.9}$$

Integrals by inspection: [****** REINSPECT THEM TOMORROW MELISSA, FOR THE LOVE OF GOD.]

$$\int 1 \, \mathrm{d}\hat{\Omega}_k = 4\pi \qquad \leftrightarrow \qquad f_1(E) \tag{K.10}$$

$$\int \left(\frac{\vec{p}\cdot\hat{k}}{E} \right) \mathrm{d}\hat{\Omega}_k = 0 \qquad \leftrightarrow \qquad f_2(E) \tag{K.11}$$

$$\int \left(\left(\frac{\vec{p}\cdot\hat{k}}{E} \right)^2 - \frac{1}{3}\frac{p^2}{E^2} \right) \mathrm{d}\hat{\Omega}_k = 0 \qquad \leftrightarrow \qquad f_3(E) \tag{K.12}$$

$$\int \left(\hat{n}\cdot\frac{\vec{p}}{E}\right) \mathrm{d}\hat{\Omega}_k \;=\; 4\pi\left(\hat{n}\cdot\tfrac{\vec{p}}{E}\right) \qquad \leftrightarrow \qquad f_4(E) \tag{K.13}$$

$$\int \left(\hat{n}\cdot\frac{\vec{p}}{E}\right)\left(\frac{\vec{p}\cdot\hat{k}}{E}\right) \mathrm{d}\hat{\Omega}_k \;=\; 0 \qquad \leftrightarrow \qquad f_5(E) \tag{K.14}$$

$$\int \left(\hat{n}\cdot\hat{k}\right) \mathrm{d}\hat{\Omega}_k \;=\; 0 \qquad \leftrightarrow \qquad f_6(E) \tag{K.15}$$

$$\int \left(\hat{n}\cdot\hat{k}\right)\left(\frac{\vec{p}\cdot\hat{k}}{E}\right) \mathrm{d}\hat{\Omega}_k \;=\; \tfrac{1}{3}4\pi\left(\hat{n}\cdot\tfrac{\vec{p}}{E}\right) \qquad \leftrightarrow \qquad f_7(E) \tag{K.16}$$

$$\int \hat{n}\cdot\left(\frac{\vec{p}\times\hat{k}}{E}\right) \mathrm{d}\hat{\Omega}_k \;=\; 0 \qquad \leftrightarrow \qquad f_8(E) \tag{K.17}$$

$$\int \hat{n}\cdot\left(\frac{\vec{p}\times\hat{k}}{E}\right)\left(\frac{\vec{p}\cdot\hat{k}}{E}\right) \mathrm{d}\hat{\Omega}_k \;=\; 0 \qquad \leftrightarrow \qquad f_9(E) \tag{K.18}$$

$$\int T_2(\hat{n}):\left[\frac{\vec{p}}{E},\frac{\vec{p}}{E}\right] \mathrm{d}\hat{\Omega}_k \;=\; 4\pi\, T_2(\hat{n}):\left[\tfrac{\vec{p}}{E},\tfrac{\vec{p}}{E}\right] \qquad \leftrightarrow \qquad f_{10}(E) \tag{K.19}$$

$$\int T_2(\hat{n}):\left[\frac{\vec{p}}{E},\frac{\vec{p}}{E}\right]\left(\frac{\vec{p}\cdot\hat{k}}{E}\right) \mathrm{d}\hat{\Omega}_k \;=\; 0 \qquad \leftrightarrow \qquad f_{11}(E) \tag{K.20}$$

$$\int T_2(\hat{n}):\left[\frac{\vec{p}}{E},\hat{k}\right] \mathrm{d}\hat{\Omega}_k \;=\; 0 \qquad \leftrightarrow \qquad f_{12}(E) \tag{K.21}$$

$$\int T_2(\hat{n}):\left[\frac{\vec{p}}{E},\hat{k}\right]\left(\frac{\vec{p}\cdot\hat{k}}{E}\right) \mathrm{d}\hat{\Omega}_k \;=\; \tfrac{1}{3}4\pi T_2(\hat{n}):\left[\tfrac{\vec{p}}{E},\tfrac{\vec{p}}{E}\right] \qquad \leftrightarrow \qquad f_{13}(E) \tag{K.22}$$

$$\int T_2(\hat{n}):\left[\hat{k},\hat{k}\right] \mathrm{d}\hat{\Omega}_k \;=\; 0 \qquad \leftrightarrow \qquad f_{14}(E) \tag{K.23}$$

$$\int T_2(\hat{n}):\left[\hat{k},\hat{k}\right]\left(\frac{\vec{p}\cdot\hat{k}}{E}\right) \mathrm{d}\hat{\Omega}_k \;=\; 0 \qquad \leftrightarrow \qquad f_{15}(E) \tag{K.24}$$

$$\int T_2(\hat{n}):\left[\frac{\vec{p}}{E},\frac{\vec{p}}{E}\times\hat{k}\right] \mathrm{d}\hat{\Omega}_k \;=\; 0 \qquad \leftrightarrow \qquad f_{16}(E) \tag{K.25}$$

$$\int T_2(\hat{n}):\left[\hat{k},\frac{\vec{p}}{E}\times\hat{k}\right] \mathrm{d}\hat{\Omega}_k \;=\; 0 \qquad \leftrightarrow \qquad f_{17}(E) \tag{K.26}$$

$$\int T_3(\hat{n}):\left[\frac{\vec{p}}{E},\frac{\vec{p}}{E},\frac{\vec{p}}{E}\right] \mathrm{d}\hat{\Omega}_k \;=\; 4\pi T_3(\hat{n}):\left[\tfrac{\vec{p}}{E},\tfrac{\vec{p}}{E},\tfrac{\vec{p}}{E}\right] \qquad \leftrightarrow \qquad f_{18}(E) \tag{K.27}$$

Appendix L

An R_{slow} Thesis Proposal

L.1 An Old Rslow Abstract

The nuclear weak force is known to be a predominantly left-handed vector and axial-vector (V-A) interaction. An experiment is proposed to further test that observation, constraining the strength of right-handed (V+A) currents by exploiting the principle of conservation of angular momentum within a spin-polarized beta decay process. Here, we focus on the decay $^{37}\mathrm{K} \rightarrow {}^{37}\mathrm{Ar} + \beta^+ + \nu_e$. The angular correlations between the emerging daughter particles provide a rich source of information about the type of interaction that produced the decay.

We obtain a sample of neutral, cold, nuclear spin-polarized ^{37}K atoms with a known spatial position, via the TRIUMF accelerator facility, by intermittently running a magneto-optical trap (MOT) to confine and cool the atoms, then cycling the trap off to polarize the atoms. With β detectors placed opposite each other along the axis of polarization, we are able to directly observe the momenta of β^+ particles emitted into 1.4% of the total solid angle nearest this axis. We also are able to extract a great deal of information about the momentum of the recoiling ^{37}Ar daughters by measuring their times of flight and hit positions on a microchannel plate detector with a delay line. Because the nuclear polarization is known to within $< 0.1\%$ [3], and we are able to account for many systematic effects by periodically reversing the polarization and by collecting unpolarized decay data while the atoms are trapped within the MOT, we expect to be well equipped to implement a test of 'handedness' within the nuclear weak force.

L.2 Motivation

The nuclear weak force has long been known to be a predominantly left-handed chiral interaction, meaning that immediately following an interaction (such as a beta decay) with a weak force carrying boson (W^+, W^-, Z), normal-matter leptons (such as the electron and electron neutrino) emerge with left-handed chirality while the anti-leptons (e.g. the positron and electron anti-neutrino) emerge with right-handed chirality. In the limit of massless particles, the particle's chirality is the same as its helicity. Thus, in a left-handed model, the direction of an (ultrarelativistic) normal lepton's spin is antiparallel direction of its motion, and the direction of spin for an anti-lepton is parallel to its direction of motion. For a non-relativistic particle the property of chirality is fairly abstract, and describes the appropriate group representation and projection operators to be used in calculations. It should be noted that a fully chiral model is also one which is maximally parity violating.

This odd quirk of the nuclear weak force is not only *predominantly* true, but it is, to the best of our current scientific knowledge, *always* true – that is, attempts to measure any right-handed chiral components of the weak force have produced results consistent with zero [1][8]. This project proposes a further measurement to constrain the strength of the right-handed component of the weak interaction.

L.3 The Principle of the Measurement

Of particular interest is the decay process: $^{37}\mathrm{K} \rightarrow {}^{37}\mathrm{Ar} + \beta^+ + \nu_e$. Among other useful properties, this is is a 'mirror' decay, meaning that the nuclear wavefunctions of the parent and daughter are identical up to their isospin quantum number. This property allows us to place strong constraints on the size of the theoretical uncertainties for this decay process within the Standard Model. We further exploit this property by noting that both the ^{37}K parent and the ^{37}Ar daughter have nuclear spin $I = 3/2$, a fact which is key to this experiment.

L.4 The Decay Process

The kinematics of nuclear β^+ decay are described by the following probability density function:

$$\begin{aligned} W(\langle I\rangle|E_\beta\hat{\Omega}_\beta\hat{\Omega}_\nu) \;=\; & \left(\frac{1}{2\pi}\right)^5 F(-Z,E_\beta)\; p_\beta E_\beta (E_0-E_\beta)^2 \mathrm{d}E_\beta \mathrm{d}\hat{\Omega}_\beta \mathrm{d}\hat{\Omega}_\nu\, \xi \left[1 + a_{\beta\nu}\frac{\vec{p}_\beta\cdot\vec{p}_\nu}{E_\beta E_\nu} + b_{\mathrm{Fierz}}\frac{m_e}{E_\beta}\right. \\ & + c_{\mathrm{align}}\left(\frac{\frac{1}{3}\vec{p}_\beta\cdot\vec{p}_\nu - (\vec{p}_\beta\cdot\hat{j})(\vec{p}_\nu\cdot\hat{j})}{E_\beta E_\nu}\right)\left(\frac{I(I+1)-3\langle(\vec{I}\cdot\hat{\imath})^2\rangle}{I(2I-1)}\right) \\ & \left. + \frac{\langle\vec{I}\rangle}{I}\left(A_\beta\frac{\vec{p}_\beta}{E_\beta} + B_\nu\frac{\vec{p}_\nu}{E_\nu} + D_{\mathrm{TR}}\frac{\vec{p}_\beta\times\vec{p}_\nu}{E_\beta E_\nu}\right)\right], \end{aligned} \tag{L.1}$$

where $\vec{I}$ is the nuclear spin-polarization, $F(-Z,E_\beta)$ is the Fermi function, and parameters ξ, $a_{\beta\nu}$, b_{Fierz}, c_{align}, A_β, B_ν, and D_{TR} are functions that vary with the strengths of the vector, axial, scalar, and tensor couplings (constant throughout nature), as well as the Fermi and Gamow-Teller nuclear matrix elements (specific to the individual decay) [9][10].

The decay may be treated as a three-body problem in which the available kinetic energy is divided up between the beta, the neutrino, and the recoiling ^{37}Ar nucleus, and (of course) the total linear and angular momentum are conserved. While the neutrino cannot be detected directly, its kinematics may be reconstructed from observations of the beta and the recoiling daughter nucleus. By placing detectors above and below the decaying atom along the axis of its polarization, we are able to obtain information about the outgoing beta's energy and momentum, in the cases of interest to us, where it is emitted along (or close to) the axis of polarization.

The recoiling ^{37}Ar nucleus is a bit trickier to work with, but the task is not impossible. One useful feature of the $^{37}\mathrm{K} \rightarrow {}^{37}\mathrm{Ar}$ transition is that, in addition to the β^+ emitted in the decay itself, one or more *orbital* electrons from the parent atom are typically lost. In the majority of decay events only one orbital electron is 'shaken off' and so the daughter ^{37}Ar atom is electrically neutral [11][12]. In the remaining cases, two or more orbital electrons are lost this way, and the daughter atom is positively charged. If we apply an electric field perpendicular to the direction of polarization, these positively charged $^{37}\mathrm{Ar}^{(+n)}$ ions may be collected into a detector, from which hit position and time of flight information may be extracted. These shake-off electrons

are emitted with an average energy of only $\sim 2\,\mathrm{eV}$ so to a very good approximation the other decay products are not perturbed by the presence of shake-off electrons.

It should be noted that for the class of decays of greatest interest, where the beta and the neutrino emerge back-to-back along the polarization axis, the recoiling daughter nucleus will have zero momentum along the directions perpendicular to this axis, and on average less total energy than if the beta and neutrino were emitted in a parallel direction. Henceforth, daughter nuclei from a back-to-back decay as shown in Figure **??** will be described as 'slow' recoils. In terms of observables, this means that if the electric field is configured to point along one of the axes perpendicular to the polarization direction, then when the recoiling ion is swept away into a detector, the slow recoil's hit position should be exactly along the projection of the polarization axis. Furthermore, the slow recoil's time of flight should be in the middle of the time of flight spectrum, since other recoils will be emitted with momentum towards or away from the detector.

L.5 Current Status

In June 2014, after several years of preparatory work beforehand (the author has been continuously involved with this project since 2010), approximately 7 days of beam time at TRIUMF was dedicated to the TRINAT ^{37}K beta decay experiment. Approximately half of this data is suitable for use in this project. During this period, approximately 10,000 atoms were held within the trap at any given time. The cleaned spectra show around 50,000 polarized beta-recoil coincidence events in total, divided among measurements at three different electric field strengths (535 V/cm, 415 V/cm, 395 V/cm).

At the present time, analysis is underway. The recoil MCP hit position data has been calibrated, and systematic effects in the trap position and size measurements are being considered. The largest two remaining hurdles for the analysis both lie in improvements to the Monte Carlo.

The first challenge is to implement particle tracking within a *non-uniform* electric field. Using the true non-uniform electric field will shift the time-of-flight spectra overall by around 1%, and is expected to change the *shape* of spectra as well, since the deviation from uniformity changes significantly as a function of flight tragectory,

and is greater the farther a particle ventures from the central axis. This would affect the measured hit positions as well. Taken together, the shape of the time-of-flight spectra (as in Figure **??**) and the recoil hit position are critical to our reconstruction of the decay process, it is critical that we model them correctly.

The second challenge will be to allow our simulation to vary vector, axial, scalar, and tensor coupling constants separately while holding other physical parameters (such as the half-life and Fermi/Gamow-Teller ratio) constant. This, too, will be absolutely critical to the analysis, and its implementation is likely to be non-trivial.

A fit to simulation has shown that the data that has already been collected has sufficient statistical power to measure the *fractional* contribution of any polarized 'new physics' beta decay parameter (ie right-handed, scalar, and tensor currents within the weak interaction) to a sensitivity of $\sim 2\%$ of its true value. Systematic limitations are still being assessed. Quantifying this observable's sensitivity to physics beyond the Standard Model in comparison to previously measured constraints [1][8] is work in progress.